Kinetic Analysis and Sequencing of Si-H and C-H Bond Activation Reactions: Direct Silylation of Arenes Catalyzed by an Iridium-Polyhydride

Miguel A. Esteruelas,* Antonio Martínez, Montserrat Oliván, and Enrique Oñate

Departamento de Química Inorgánica – Instituto de Síntesis Química y Catálisis Homogénea (ISQCH) – Centro de Innovación en Química Avanzada (ORFEO-CINQA), Universidad de Zaragoza – CSIC, 50009 Zaragoza, Spain

ABSTRACT: The saturated trihydride $IrH_3\{\kappa^3$-P,O,P-[xant(P^iPr_2)$_2$]} (**1**; xant(P^iPr_2)$_2$ = 9,9-dimethyl-4,5-bis(diisopropylphosphino)xanthene) coordinates the Si-H bond of triethylsilane, 1,1,1,3,5,5,5-heptamethyltrisiloxane, and triphenylsilane to give the σ-complexes $IrH_3(\eta^2$-H-$SiR_3)\{\kappa^2$-*cis*-P,P-[xant(P^iPr_2)$_2$]}, which evolve to the dihydride-silyl derivatives $IrH_2(SiR_3)\{\kappa^3$-P,O,P-[xant(P^iPr_2)$_2$]} (SiR_3 = $SiEt_3$ (**2**), $SiMe(OSiMe_3)_2$ (**3**), $SiPh_3$ (**4**)) by means of the oxidative addition of the coordinated bond and the subsequent reductive elimination of H_2. Complexes **2-4** activate a C-H bond of symmetrically and asymmetrically substituted arenes to form silylated arenes and to regenerate **1**. This sequence of reactions defines a cycle for the catalytic direct C-H silylation of arenes. Stoichiometric isotopic experiments and the kinetic analysis of the transformations demonstrate that the C-H bond rupture is the rate determining step of the catalysis. As consequence, the selectivity of the silylation of substituted arenes is generally governed by ligand-substrate steric interactions.

INTRODUCTION

Transition metal-mediated cross-coupling reactions involving elemental steps of σ-bond activation in both substrates (Scheme 1) are challenging from a conceptual point of view. The reason is the need of sequencing the split of the σ-bonds in the metal coordination sphere, which requires an adequate difference between the activation energies of the bond rupture reactions. Thus, the success of the cross-coupling demands the control of the sequencing process, for which it is necessary to know and to govern such parameters. The latter is achieved by having a deep knowledge of what is happening just before the σ-bond cleavage step. It is generally assumed that the first step for a σ-bond activation reaction is the coordination of the σ-bond to the metal center of an unsaturated compound. The interaction involves σ-donation from the σ-orbital of the bond to empty orbitals of the metal and back bonding from the metal to the σ* orbital of the bond.[1]

Scheme 1. General Scheme for Cross-Coupling Reactions Involving Two σ-Bond Activations

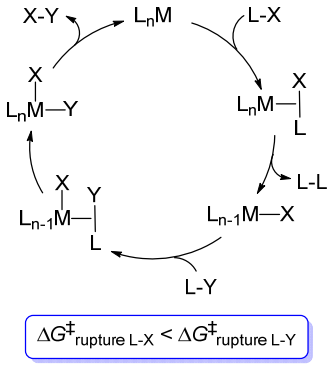

The intermolecular C-H silylation of arenes without the use of directing groups is a particular type of this class of cross-coupling reactions of great interest. The silylated products are useful precursors to commercial polymers and copolymers and can be also used as intermediates for organic synthesis. The reactions are environmentally friendlier than the classical procedures of synthesis of arylsilanes, minimizing waste formation, and offer the possibility of reaching alternative regioselectivities.[2] The catalysis involves the activation of the Si-H bond of the silane[3] and a C-H bond of the arene,[4] before the coupling of the substrates. Although transition metal-silyl derivatives are a prominent group of compounds, comparable in relevance to the aryl derivatives, there is significantly less information on silane Si-H bond splitting than on the arene C-H bond activation. Two features distinguish silicon from carbon and hydrogen, its higher electropositive character and the hypervalent ability. As a consequence, a greater variety of interactions M-HSi than M-HC has been proposed, while a consensus as to how to distinguish between them has not yet been reached.[3b,5] Much effort has been centered in the stabilization and characterization of these interactions, whereas the H-Si cleavage process has received less attention. Often, M-HSi compounds are treated as still pictures of a situation more than as transitory species on the way to the Si-H activation.[6]

Catalysts for the arene C-H silylation include complexes of ruthenium,[7] rhodium,[8] iridium,[9] nickel,[10] platinum,[11] and some rare-earth.[12] Knowledge on the identity of species by which the catalysts functionalize the C-H bond is scarce. Recently, it has been proposed that the iridium systems generated from $[Ir(\mu$-OMe)(η^4-COD)]$_2$ (COD = 1,5-cyclooctadiene) and phenanthroline ligands work through only one cycle involving both dihydride-silyl and hydride-disilyl complexes (Scheme 2). In a sequential manner the former activates the Si-H bond

of the silane, whereas the second adds a C-H bond of the arene to subsequently promote the silyl-aryl coupling.[9n]

Scheme 2. Dihydride-Silyl and Hydride-Disilyl Mediated Silylation of Arenes

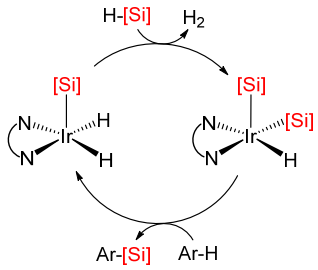

[Si] = $SiMe(OSiMe_3)_2$

The ligands used for stabilizing C-H silylation catalysts are usually monodentate and bidentate. Pincer ligands are having a tremendous impact in current catalysis because of their ability for stabilizing uncommon species, which open novel approaches.[13] However, they have been scarcely used for supporting these catalysts. As far as we know, only one catalyst bearing a ligand of this class has been previously employed. In 2007, Tilley and co-workers reported that complex Ir(κ^3-NSiN)H(OTf)(COE) (NSiN = bis(8-quinolyl)methylsilyl, OTf = triflate, COE = cyclooctene) is active for arylsilane redistribution and for the dehydrogenative silylation of arenes.[14]

9,9-Dimethyl-4,5-bis(diisopropylphosphino)xanthene (xant(P^iPr_2)$_2$) is an ether-diphosphine which has demonstrated to have a higher capacity than other POP-diphosphines to act as pincer.[15] However, its flexibility along with the hemilabile character of the ether function allows it to adapt to the requirements of the participating intermediates of the catalytic cycles.[16] As proof-of-concept, species bearing the diphosphine coordinated in κ^3-*mer*,[17] κ^3-*fac*,[18] κ^2-*cis*,[19] and κ^2-*trans*[20] fashions have been isolated, whereas notable catalysts of platinum group metals stabilized by this ligand have proved to be efficient for a wide range of reactions. For the elements of iron triad, it should be mentioned the ruthenium complex RuH(η^2-H_2BH_2)\{κ^3-P,O,P-[xant($PiPr_2$)$_2$]\}, which is an efficient catalyst precursor for the hydrogen transfer from 2-propanol to ketones, the α-alkylations of phenylacetonitrile and acetophenone with alcohols, and the regio- and stereoselective head-to-head (*Z*)-dimerization of terminal alkynes,[21] whereas the osmium-tetrahydride OsH_4\{κ^3-P,O,P-[xant($PiPr_2$)$_2$]\} also catalyzes the latter[22] and the hydroxo-osmium(IV) derivative $OsH_3(OH)$\{κ^3-P,O,P-[xant($PiPr_2$)$_2$]\} dehydrogenates formic acid to H_2 and CO_2.[23] Reactions catalyzed by rhodium complexes include: dehydropolymerization of $H_3B{\cdot}NMeH_2$,[24] dehydrogenation of ammonia borane[25] and alkanes,[26] monoalcoholysis of diphenylsilane,[27] borylation of arenes,[28] decyanative borylation of nitriles,[29] borylation of alkynes,[30] dehalogenation of chloroalkanes, and homocoupling of benzyl chloride.[31] Recently, we have observed that the iridium-trihydride IrH_3\{κ^3-P,O,P-[xant(P^iPr_2)$_2$]\} catalyzes the direct borylation of arenes with the help of dihydride-boryl and hydride-diboryl derivatives. The three compounds are involved in two catalytic cycles, which have the dihydride-boryl complex as common intermediate because of its ability to activate both B-H and C-H bonds (Scheme 3).[32]

Scheme 3. Mechanism for the Borylation of Arenes catalyzed by the trihydride IrH_3\{κ^3-P,O,P-[xant(P^iPr_2)$_2$]\}

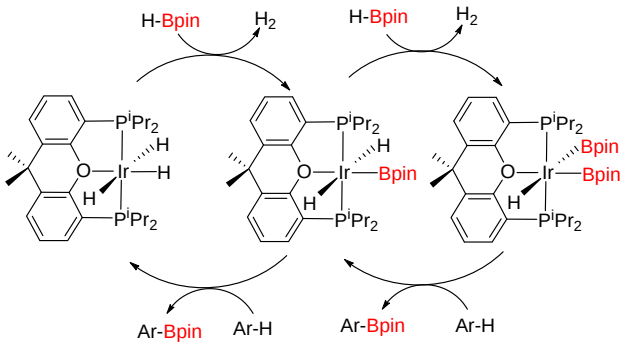

The diagonal relationship between the elements of rows 2 and 3 is well known, being particularly marked for boron and silicon.[33] With that in mind, we reasoned that complex IrH_3\{κ^3-P,O,P-[xant(P^iPr_2)$_2$]\} should be also an efficient catalysts for the silylation of arenes. Thus, in order to build a catalytic cycle for the arene C-H silylation, related to those shown to Scheme 3, we decided to study the activation of the Si-H bond of silanes promoted by this trihydride and the C-H bond activation of arenes promoted by the resulting silyl products, paying particular attention to the kinetics of the processes and to the reaction intermediates. This paper demonstrates that the iridium-promoted arene C-H silylation can also take place through trihydride and dihydride-silyl complexes without the help of hydride-disilyl species.

RESULTS AND DISCUSSION

Si-H Bond Activation. As expected for the diagonal relationship between boron and silicon, trihydride complex IrH_3\{κ^3-P,O,P-[xant(P^iPr_2)$_2$]\} (**1**) activates the Si-H bond of silanes such as triethylsilane, 1,1,1,3,5,5,5-heptamethyltrisiloxane, and triphenylsilane (Scheme 4). Treatment of toluene solutions of **1** with 1.0 equiv of the silanes, at room temperature, for 18 h leads to the corresponding dihydride-silyl derivatives $IrH_2(SiR_3)$\{κ^3-P,O,P-[xant(P^iPr_2)$_2$]\} (SiR_3 = $SiEt_3$ (**2**), $SiMe(OSiMe_3)_2$ (**3**), $SiPh_3$ (**4**)) and molecular hydrogen. Complexes **2-4** were isolated as white solids in 49-55% yield.

Complex **3** was characterized by X-ray diffraction analysis. The structure, which has two molecules chemically equivalent but crystallographically independent in the asymmetric unit (Figure 1 shows one of them), reveals a disposition *trans* for the hydride ligands (H(01)-Ir(1)-H(02) = 173(7) and 169(7)). The coordination polyhedron around the iridium center can be rationalized as a distorted octahedron with the ether-diphosphine coordinated in a *mer* fashion (P(1)-Ir(1)-P(2) = 156.82(15)º and 161.33(14)º, P(1)-Ir(1)-O(3) = 82.0(3)º and 81.1(3)º, and P(2)-Ir(1)-O(3) = 81.5(3)º and 81.3(3)º) and the silyl group located *trans* to the diphosphine oxygen atom (Si(1)-Ir(1)-O(3) = 170.4(3)º and 172.8(3)º). The Ir(1)-Si(1) bond lengths of 2.262(4) Å and 2.271(4) Å compare well with those reported for other iridium(III)-silyl complexes.[34] The ^1H, $^{31}P\{^1H\}$ and $^{29}Si\{^1H\}$ NMR spectra of **2-4**, in benzene-d_6, at room temperature are consistent with the structure shown in Figure 1. In the ^1H NMR spectra, the most noticeable feature is the resonance corresponding to the equivalent hydrides, which appears as a triplet ($^2J_{H\text{-}P}$ = 17 Hz) between -5.2 and -6.2 ppm. The $^{31}P\{^1H\}$ NMR spectra show a singlet between 44 and 54 ppm, in agreement with equivalent P^iPr_2 moieties. The

Scheme 4. Reactions of 1 with Silanes

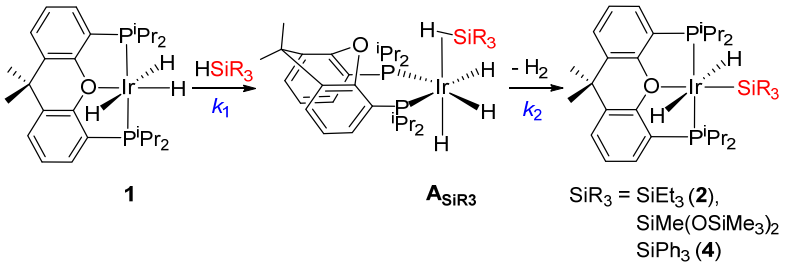

$^{29}Si\{^{1}H\}$ NMR spectra contain an Ir-Si resonance, which is observed as a triplet ($^{2}J_{Si\text{-}P}$ = 10 Hz) between -9 and -59 ppm.

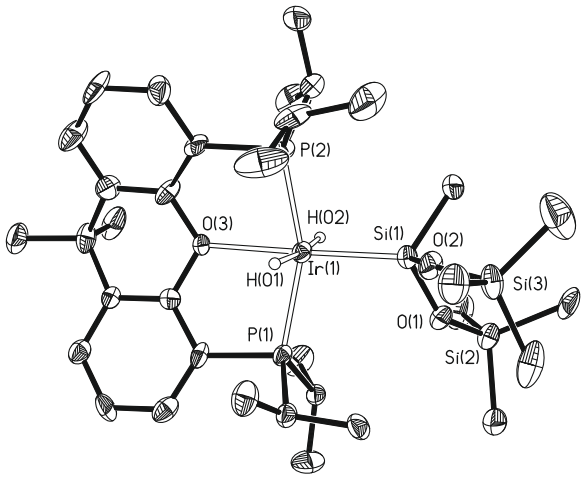

Figure 1. Molecular diagram of complex **3** (ellipsoids shown at 50% probability). All hydrogen atoms (except the hydrides) are omitted for clarity. Selected bond distances (Å) and angles (deg): Ir(1)-P(1) = 2.252(4), 2.245(4), Ir(1)-P(2) = 2.263(4), 2.262(4), Ir(1)-O(3) = 2.339(9), 2.324(9), Ir(1)-Si(1) = 2.262(4), 2.271(4); P(1)-Ir(1)-P(2) = 156.83(15), 161.33(14), P(1)-Ir(1)-O(3) = 82.0(3), 81.1(3), P(2)-Ir(1)-O(3) = 81.5(3), 81.4(3), P(1)-Ir(1)-Si(1) = 98.91(15), 98.00(15), P(2)-Ir(1)-Si(1) = 100.05(15), 100.18(16), H(01)-Ir(1)-H(02) = 173(7), 169(7), Si(1)-Ir(1)-O(3) = 170.4(3), 172.8(3).

The monitoring of the activations by ^{1}H and $^{31}P\{^{1}H\}$ NMR spectroscopy in toluene-d_8 reveals that the reactions are quantitative and take place via the intermediates $\mathbf{A_{SiR3}}$ shown in Scheme 4. At room temperature, characteristic features of these transitory species are a broad hydride resonance centered between -11.2 and -12.2 ppm in the ^{1}H NMR spectra and a broad signal centered between -1 and -5 ppm in the $^{31}P\{^{1}H\}$ NMR spectra. The half-live of these intermediates depends upon the substituents attached to the silicon atom, increasing in the sequence $SiPh_3$ < $SiMe(OSiMe_3)_2$ < $SiEt_3$. The half-live of intermediate $\mathbf{A_{SiEt3}}$ is long enough to allow its spectroscopic study at 183 K. Figure 2 collects the most informative NMR spectra at this temperature. The $^{31}P\{^{1}H\}$ NMR spectrum (a) shows two doublets ($^{2}J_{P\text{-}P}$ = 18 Hz) at 8.7 (a^1) and -5.9 (a^2) ppm and a broad singlet at -12.8 (b^1) ppm. The COSY $^{31}P\text{-}^{31}P$ spectrum (b) confirms that the doublets correspond to the same molecule (**A**), which bears a κ^2-P,P-*cis*-diphosphine with inequivalent P^iPr_2 groups, whereas the broad singlet represents other κ^2-P,P-*cis*-diphosphine species with chemically equivalent P^iPr_2 moieties (**B**) The molar ratio between them is approximately 2:1. The HMBC $^{31}P\text{-}^{1}H$ spectrum (c) reveals hydride resonances for **A** at -9.7 (a_1), -11.2 (a_2), -12.6 (a_3), and -14.4 (a_4) ppm, whereas those of **B** appear at -9.7 (b_1), -10.0 (b_2), and -14.2 (b_3+b_4) ppm. According to an **A**:**B** molar ratio of 2:1, the $^{1}H\{^{31}P\}$ spectrum in the high field region (Figure S19) displays an a_1+b_1:b_2:a_2:a_3:b_3+b_4:a_4 intensity ratio of 3:1:2:2:2:2. Furthermore, on the basis of this spectrum and the ^{1}H one, a *trans* disposition of the hydrides corresponding to resonances a_3 and a_4 and the P^iPr_2 groups of **A** ($^{2}J_{H\text{-}P}$ = 104 and 113 Hz, respectively), and between the hydrides assigned to signal b_3+b_4 and the P^iPr_2 moieties of **B**, can be deduced. The signal b_3+b_4 is the AA' part of an AA'XX' spin system with $^{2}J_{A\text{-}X}$ = $^{2}J_{A'\text{-}X'}$ = 116 Hz. The decoupling of the ^{31}P nucleus brings to light hidden ^{29}Si satellites on the signal a_2. At the first glance, the $^{1}J_{H\text{-}Si}$ value of 43 Hz suggests some degree of Si-H interaction and the formation of a "*symmetric oxidative addition product*".[35] The Si-H interaction in **A** and the value of the $^{1}J_{H\text{-}Si}$ is also supported by the HMQC $^{29}Si\text{-}^{1}H$ spectrum (d), which contains the cross-spot between the resonance a_2 and the Ir-Si resonance, which is observed at 2.8 ppm in the $^{29}Si\{^{1}H\}$ NMR spectrum. This bidimensional spectrum also is consistent with Si-H interaction in **B**, showing a cross-spot between Ir-Si and b_1 resonances, although the value of $^{1}J_{H\text{-}Si}$ cannot be measured in this case. All these spectroscopic features together suggest that $\mathbf{A_{SiEt3}}$ exists in solution as a mixture of two species, **A** and **B**, which have structures resembling to that calculated by Schley and co-workers for the compound $IrH_4(SiEt_3)(PPh_3)_2$;[36] i. e., an octahedron formed by the diphosphine κ^2-*cis*-P,P coordinated, three hydrides *fac*-disposed, and the Si-H bond situated *trans* to a hydride. Optimization of this structure by DFT calculations (see Supporting Information) shows the silicon atom in position *anti* with regard to the oxygen of the diphosphine. Keeping this disposition there are several rotamers involving the alkyl substituents of the diphosphine and silane. The isopropyl substituents of the P^iPr_2 groups can be disposed in positions eclipsed or alternating, which gives rise to structures bearing equivalent or inequivalent P^iPr_2 groups, in agreement with the spectroscopic observations. The disposition of the isopropyl groups slightly modifies the position of the silicon atom, which changes the P-Ir-Si angles.

The criterion of the value of $^{1}J_{H\text{-}Si}$ is ambiguous to establish the nature of the Si-H interaction. So, we decided to prepare a monodeuterated $\mathbf{A_{SiEt3}}$ species, by reaction of **1** with Et_3SiD, after reasoning that the rupture of the Si-D bond should give

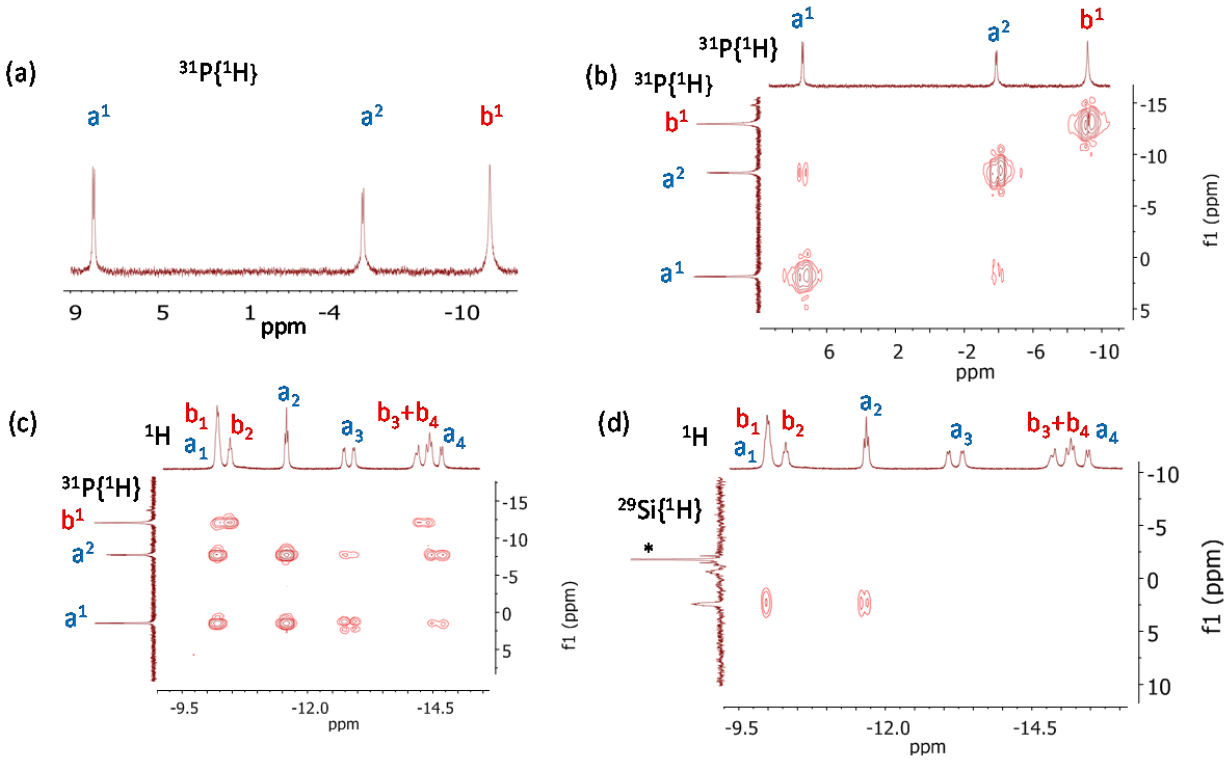

Figure 2. (a) $^{31}P\{^{1}H\}$ NMR spectrum (202.46 MHz, C_7D_8, 183 K); (b) ^{31}P-^{31}P COSY spectrum (202.46 MHz, C_7D_8, 183 K); (c) HMBC $^{31}P\{^{1}H\}$-^{1}H NMR spectrum (202.46/500.13 MHz, C_7D_8, 183 K); and (d) HMQC ^{29}Si-^{1}H NMR spectrum (99.36/500.13 MHz, C_7D_8, 183 K; * denotes excess of $HSiEt_3$) of $\mathbf{A_{SiEt3}}$.

rise to deuterium distribution between all hydride positions, since at room temperature the six signals observed at 183 K coalesce to give only one, while if the Si-D bond was maintained only the intensities of resonances b_1 and a_2 should be modified. The high field region of the ^{1}H and ^{2}H NMR spectra of the monodeuterated $\mathbf{A_{SiEt3}}$ intermediate at 183 K (Figure 3) clearly support the second possibility; i.e., $\mathbf{A_{SiR3}}$ are species on the way to the rupture of the Si-H bond.

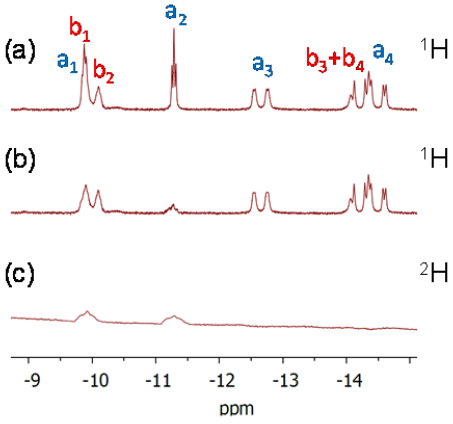

Figure 3. High field region of the ^{1}H NMR spectra at 183 K of $\mathbf{A_{SiEt3}}$ (500 MHz, toluene-d_8) (a), and $\mathbf{A_{SiEt3\text{-}d}}$ (b), and of the ^{2}H NMR spectrum (76.77 MHz, toluene) of $\mathbf{A_{SiEt3\text{-}d}}$ (c).

Having clarified the nature of the $\mathbf{A_{SiR3}}$ intermediates, we subsequently analyzed the deuterium present in the final product from the reaction of **1** with $DSiEt_3$, finding about 12% of deuterium in the hydride positions (Figure S20). It is a 75:25 mixture of isotopomers **2** and **2-d_1** (Scheme 5). The presence of **2** in the mixture indicates that the creation of a coordination vacancy in **1** by reductive elimination of molecular hydrogen does not occur, in spite of its saturated character. Such reductive elimination takes place after the Si-D rupture. Furthermore, the lower percentage of **2-d_1** in the mixture is consistent with a rapid reductive elimination, which is only governed by the H-D bond energy. The rate determining step of the overall Si-H bond activation process is the Si-H bond rupture. According to this a significant slowdown of the reaction is also observed by changing $HSiEt_3$ by $DSiEt_3$.

Scheme 5. Reaction of 1 with $DSiEt_3$.

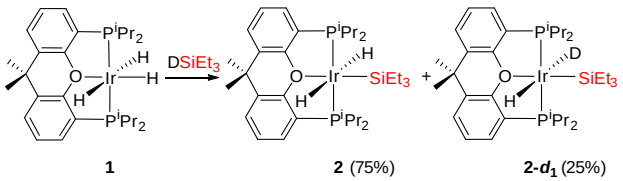

The isotope labeling experiments previously mentioned only provide a qualitative picture of the Si-H bond activation promoted by **1**. In order to gain quantitative insight of the process, the kinetic study of the reaction sequence shown in Scheme 4 was carried out. 1,1,1,3,5,5,5-Heptamethyltrisiloxane was selected as model of silane because the half-life of the $\mathbf{A_{SiMe(OSiMe3)2}}$ species is intermediate between those of $\mathbf{A_{SiPh3}}$

Table 1. Rate Constants for the Transformations of 1 into $A_{SiMe(SiOMe3)2}$ (k_1^{obs} and k_1, calculated according to eqs 1 and 4, respectively) and of $A_{SiMe(SiOMe3)2}$ into 3 (k_2, calculated according to eq 3)

T (K)	$[\mathbf{1}]_o$ (M)	[HSi] (M)	[DSi] (M)	k_1^{obs} x 10^{-4} (s^{-1})	k_1 x 10^{-4} ($M^{-1}\cdot s^{-1}$)	k_2 x 10^{-5} (s^{-1})
278	0.037	1.12	-	(0.63 ± 0.07)	(0.56 ± 0.07)	(0.49 ± 0.04)
283	0.037	1.12	-	(1.36 ± 0.06)	(1.21 ± 0.06)	(1.14 ± 0.10)
288	0.037	1.12	-	(2.34 ± 0.04)	(2.09 ± 0.04)	(2.36 ± 0.11)
293	0.037	1.12	-	(4.12 ± 0.10)	(3.68 ± 0.10)	(4.36 ± 0.04)
298	0.037	1.12	-	(7.53 ± 0.08)	(6.72 ± 0.08)	(9.07 ± 0.07)
288	0.037	-	1.12	(2.02 ± 0.05)	(1.80 ± 0.05)	(1.03 ± 0.10)
293	0.037	-	1.12	(3.52 ± 0.08)	(3.14 ± 0.08)	(1.77 ± 0.09)
298	0.037	-	1.12	(6.49 ± 0.07)	(5.79 ± 0.07)	(3.78 ± 0.12)
288	0.037	0.76	-	(1.41 ± 0.10)	(1.86 ± 0.10)	(2.32 ± 0.07)
288	0.037	0.95	-	(1.81 ± 0.06)	(1.91 ± 0.06)	(2.43 ± 0.10)
288	0.037	1.33	-	(2.51 ± 0.08)	(1.88 ± 0.08)	(2.45 ± 0.09)
288	0.037	1.52	-	(2.81 ± 0.07)	(1.85 ± 0.07)	(2.33 ± 0.07)

and A_{SiEt3}. The study was performed by $^{31}P\{^1H\}$ NMR spectroscopy, in toluene, under pseudo-first order conditions using silane concentrations between 0.76 and 1.52 M, for an initial concentration of **1** ($[\mathbf{1}]_0$) of 0.037 M, and a temperature range 278−298 K. Figure 4 shows the $^{31}P\{^1H\}$ spectrum of the reaction mixture, as a function of the time, at 288 K, for a concentration of silane of 1.12 M.

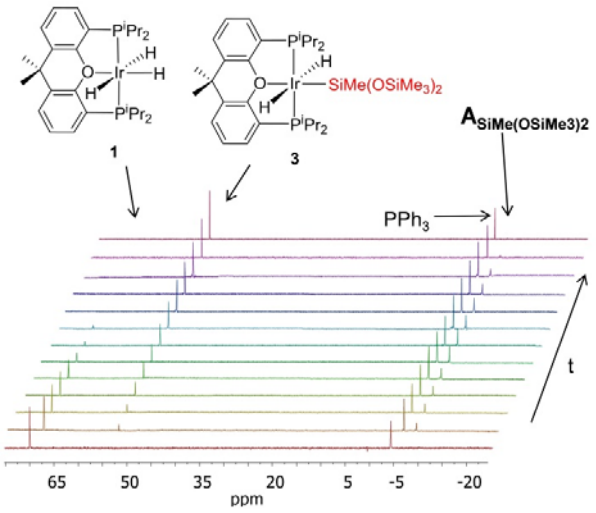

Figure 4. Stacked $^{31}P\{^1H\}$ NMR spectra (121.4 MHz, toluene, 288 K) showing the course of the reaction of **1** with 1.12 M of $HSiMe(OSiMe_3)_2$ (PPh_3 used as internal standard).

The dependence of the amounts of **1**, $\mathbf{A_{SiMe(OSiMe3)2}}$, and **3** with the time (Figure 5) is as expected for two consecutive irreversible reactions and fits to eqs 1-3, respectively. [37]

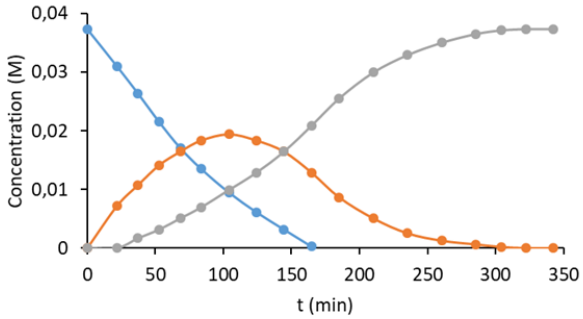

Figure 5. Composition of the mixture as a function of time for the reaction of 0.037 M of **1** with 1.12 M of $HSiMe(OSiMe_3)_2$ at 298 K: **1** (blue •), $\mathbf{A_{SiMe(OSiMe3)2}}$ (orange •), **3** (grey •).

$$[\mathbf{1}] = [\mathbf{1}]_0\, e^{-k_1^{obs}t} \qquad (1)$$

$$[\mathbf{A_{SiMe(OSiMe3)2}}] = \frac{[\mathbf{1}]_0\, k_1^{obs}}{k_2 - k_1^{obs}}\left[e^{-k_1^{obs}t} - e^{-k_2\, t}\right] \qquad (2)$$

$$[\mathbf{3}] = [\mathbf{1}]_0 + \frac{[\mathbf{1}]_0}{k_1^{obs} - k_2}\left[k_2\, e^{-k_1^{obs}t} - k_1^{obs} e^{-k_2\, t}\right] \qquad (3)$$

where

$$k_1^{obs} = k_1\,[HSiMe(OSiMe_3)_2] \qquad (4)$$

Values of k_1^{obs}, k_1, and k_2, for each temperature, obtained from these expressions are collected in Table 1. A plot k_1^{obs} vs $[HSiMe(SiOMe_3)_2]$ (Figure 6) provides a value of 1.89 ± 0.1 x 10^{-4} $M^{-1}\cdot s^{-1}$ for k_1 at 288 K, whereas the value of k_2 at this temperature is 2.38 ± 0.7 x 10^{-5} s^{-1}. The activation parameters for the coordination of the silane, calculated from the corresponding Eyring analysis (Figure 7), are $\Delta H_1^{\ddagger}$ = 19.5 ± 2.1 kcal·mol^{-1} and $\Delta S_1^{\ddagger}$ = -7.5 ± 3.4 cal·K^{-1}·mol^{-1}. These values yield an activation energy $\Delta G_1^{\ddagger}$ at 298 K of 21.7 ± 3.1

kcal·mol^{-1}. The Eyring analysis for the transformation from $\mathbf{A_{SiMe(OSiMe3)2}}$ to **3** (Figure 8) gives values of $\Delta H_2^{\ddagger} = 23.1 \pm 2.4$ kcal·mol^{-1} and $\Delta S_2^{\ddagger} = 0.5 \pm 3.1$ cal·K^{-1}, which afford an activation energy $\Delta G_2^{\ddagger}$ at 298 K of 23.0 ± 3.3 kcal·mol^{-1}·mol^{-1}.

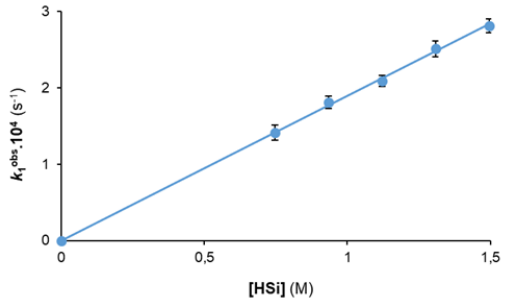

Figure 6. Plot of k_1^{obs} *versus* [HSiMe(OSiMe$_3$)$_2$].

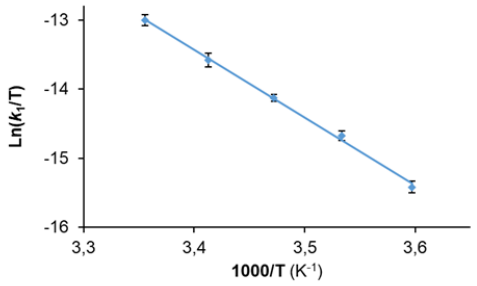

Figure 7. Eyring plot for the transformation of **1** into $\mathbf{A_{SiMe(SiOMe3)2}}$.

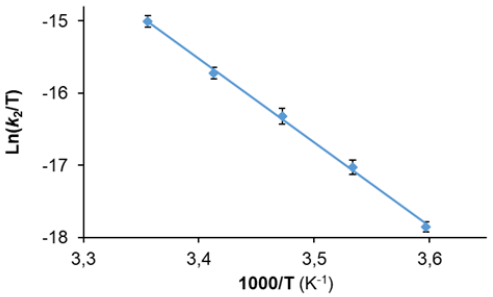

Figure 8. Eyring plot for the transformation of $\mathbf{A_{SiMe(SiOMe3)2}}$ into **3**.

The negative value of the activation entropy for the formation of $\mathbf{A_{SiMe(OSiMe3)2}}$ is consistent with the intermolecular character of the process and suggests an ordered transition state involving the participation of the silane. Because complex **1** is saturated and the coordination of the Si-H bond requires the κ^3-to-κ^2 change in the coordination of the diphosphine, by dissociation of the hemilabile oxygen, that entropy value points out in favor of an hypervalent hydride-silicon interaction previous to the oxygen dissociation. Such interaction, which is broken in the coordination, should decrease the activation energy of the dissociation. The value of the activation entropy for the transformation from $\mathbf{A_{SiMe(OSiMe3)2}}$ to **3**, close to zero, is in agreement with the fast nature of the elimination of molecular hydrogen and points out the Si-H rupture as rate determining step. Table 1 also contains values of the rate constants $k_1^{obs\text{-}d}$ and k_2^{d} obtained for reactions with DSiMe(OSiMe$_3$)$_2$. The ratio $k_1^{obs}/k_1^{obs\text{-}d}$ of 1.16 ± 0.01 confirms that the silane has not a direct participation in the rate-determining transition state for the transformation of **1** into $\mathbf{A_{SiMe(OSiMe3)2}}$, although it is present. In contrast, the ratio k_2/k_2^{d} gives a primary isotope effect of 2.40 ± 0.11, which corroborates the rupture of the Si-H bond as the rate determining step for the formation of **3**.[38]

Scheme 6 summarizes the Si-H bond activation of silanes promoted by the trihydride **1**, on the basis of the previously mentioned results. The silane-assisted dissociation of the hemilabile ether of the diphosphine affords the unsaturated intermediates **I**, which subsequently coordinate the silane to give $\mathbf{A_{SiR3}}$. The oxidative addition of the coordinated Si-H bond, in the rate determining step, leads to **II**. The latter rapidly eliminates molecular hydrogen to give **III**. Finally, the recoordination of the diphosphine ether group yields **2-4**.

Scheme 6. Si-H Bond Activation of Silanes Promoted by 1.

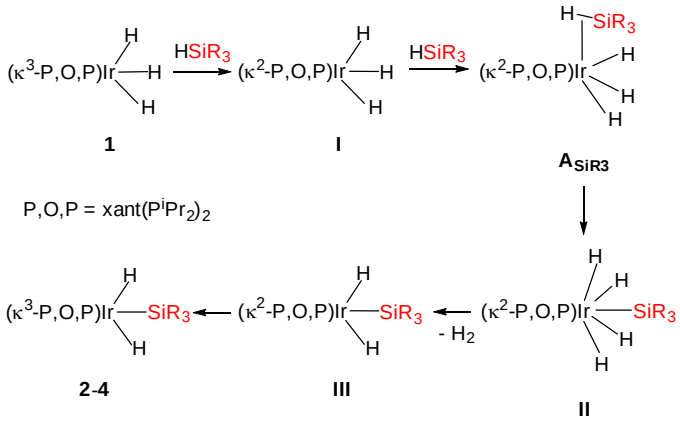

C-H bond Activation. Dihydride-silyl complexes **2-4** react in benzene solution to give R$_3$Si-Ph and the trihydride derivative **1** (Scheme 7).

Scheme 7. Reactions of Complexes 2-4 with Benzene

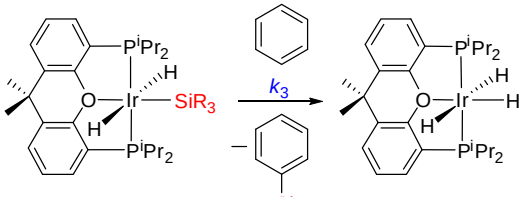

SiR$_3$ = SiEt$_3$ (**2**), SiMe(OSiMe$_3$)$_2$ (**3**), SiPh$_3$ (**4**)

The transformation from **3** to **1** was followed by $^{31}P\{^1H\}$ NMR spectroscopy as a function of the time between 333 and 353 K. The decrease of **3** with the corresponding increase of **1** (Figure S1) is an exponential function of the time, fitting to an expression of first-order:

$$ln\frac{[\mathbf{3}]}{[\mathbf{3}]_0} = -k_3 t \qquad (5)$$

where $[\mathbf{3}]_0$ and [**3**] are the concentrations of **3** at the initial time and time *t*, respectively. The values obtained for k_3 are collected in Table 2. The activation parameters obtained from the Eyring analysis (Figure 9) are $\Delta H_3^{\ddagger}$ = 23.2 ± 2.2 kcal·mol^{-1}

and $\Delta S_3^{\ddagger}$ = -12.2 ± 2.9 cal·K^{-1}·mol^{-1}. These values yield an activation energy $\Delta G_3^{\ddagger}$ at 298 K of 26.8 ± 3.0 kcal·mol^{-1}. The rate of the reaction of **3** with benzene-d_6 is significantly slower than that with benzene. The ratio k_3/k_3^{d} gives a primary isotope effect of 3.1 ± 0.1, which supports the rupture of the aromatic C-H bond as the rate determining step of the coupling.

Table 2. Rate Constants for the transformation of 3 into 1 (k_3)

T (K)	$[\mathbf{3}]_o$ (M)	Arene	k_3 x 10^{-5} (s^{-1})
333	0.037	C_6H_6	0.81 ± 0.08
338	0.037	C_6H_6	1.49 ± 0.07
343	0.037	C_6H_6	2.71 ± 0.10
348	0.037	C_6H_6	3.92 ± 0.07
353	0.037	C_6H_6	6.41 ± 0.05
343	0.037	C_6D_6	0.88 ± 0.08

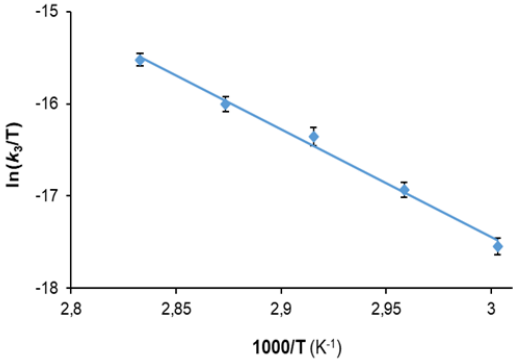

Figure 9. Eyring plot for the transformation of **3** into **1**.

These results are consistent with a classical mechanism for the C-H bond activation of the arene, which can be summarized according to Scheme 8. The coordination of the organic substrate to the metal center of the unsaturated intermediates **III** shown in Scheme 6 should give the σ-derivatives **IV**, which would evolve to **V** by oxidative addition of the coordinated C-H bond. The rapid reductive elimination of the functionalized product should lead to **I**, which could regenerate **1** by coordination of the diphosphine ether group.

Scheme 8. Proposed Mechanism for the C-H Bond Activation of Arenes

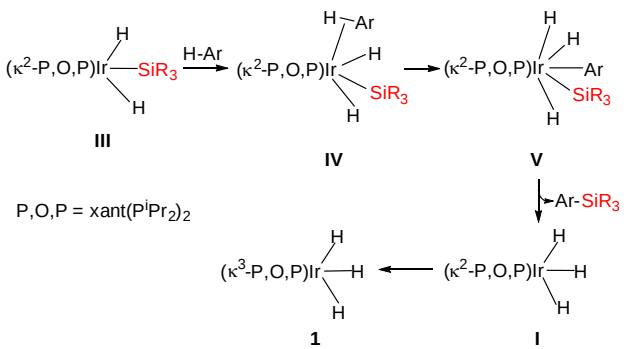

Catalytic Cross-Coupling: Silylation of Arenes. The sequencing of reactions summarized in Schemes 4 and 7 gives rise to a cycle as that shown in Scheme 1, which is different from those summarized in Schemes 2 and 3. The sequencing is possible because there is a suitable difference between the activation energies of the Si-H and C-H bond activation processes of 1,1,1,3,5,5,5-heptamethyltrisiloxane and benzene, respectively ($\Delta G_2^{\ddagger} < \Delta G_3^{\ddagger}$). According to this, complex **1** catalyzes the cross-coupling between the silane and arenes to afford functionalized arenes and molecular hydrogen (Scheme 9).

Scheme 9. Mechanism for the Silylation of Arenes

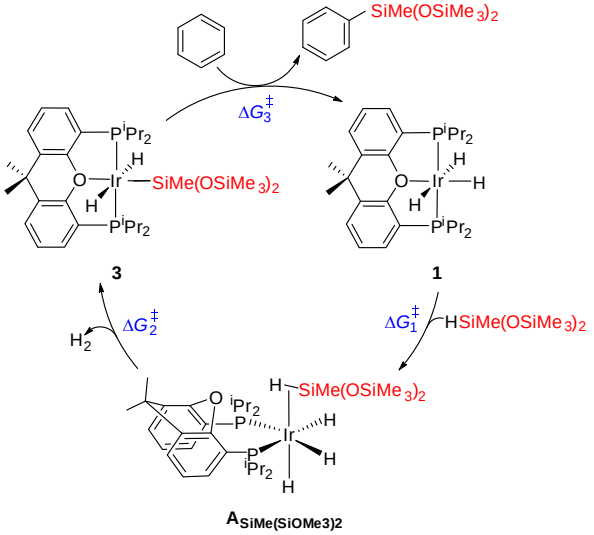

$\Delta G_1^{\ddagger}$ at 298 K = 21.7 ± 3.1 kcal·mol^{-1}
$\Delta G_2^{\ddagger}$ at 298 K = 23.0 ± 3.3 kcal·mol^{-1}
$\Delta G_3^{\ddagger}$ at 298 K = 26.8 ± 3.0 kcal·mol^{-1}

The catalysis was carried out at 110 ºC, using the arene as solvent, since the rate determining step for the cross-coupling is the rupture of a C-H bond of the arene, according to the activation energy values collected in Scheme 9. Furthermore, because complexes **2**-**4** regenerate **1** and the silane under hydrogen atmosphere and complex **1** also catalyzes the hydrogenation of olefins faster than the arene silylation,[32] cyclohexene in a silane:olefin 1:1 molar ratio was employed as hydrogen acceptor. Under these conditions, complex **1** promotes the silylation of benzene and mono- and disubstituted benzenes..

The behavior of the trihydride **1** during the silylation of benzene was followed by $^{31}P\{^{1}H\}$ NMR, to gain insight into the one pot functionalization. Figure 10 shows the $^{31}P\{^{1}H\}$ spectrum of the catalytic mixture as a function of the time. In agreement with the cycle shown in Scheme 9, including the activation energies of the stoichiometric reactions, trihydride **1** is initially transformed into the dihydride-silyl complex **3**, which is the only one detected species while the silane is present in the solution. Once the silane is consumed, complex **3** quantitatively regenerates the trihydride **1**. Any hydride-disilyl derivative related to those shown in Scheme 2 or analogous to the hydride-diboryl compound collected in Scheme 3 is not observed. The presence of **3** during the catalysis, as main metal species, strongly supports that the C-H bond cleavage of the arene is the rate determining step of the functionalization,

as expected for the fact of that the stoichiometric reaction of **3** with benzene has the highest activation energy from the stoichiometric reactions involved in cycle shown in Scheme 9. In order to have an additional evidence of that the cycle of Scheme 9 operates under catalytic conditions; we determined the activations parameters for the benzene silylation under one-pot conditions. The values of k_{cat}^{obs} collected in Table 3 were calculated by measuring the decrease of the amount of silane in the ^{1}H NMR spectrum of the catalytic solution as a function of the time, starting from an initial silane concentration of 0.28 M and a concentration of **1** of 0.028 M, in the temperature range 338-353 K. The corresponding Eyring analysis (Figure 11) yields values of $\Delta H_{cat}^{\ddagger}$ = 24.1 ± 2.6 kcal·mol^{-1}, $\Delta S_{cat}^{\ddagger}$ = -11.6 ± 3.2 cal·K^{-1}·mol^{-1}, and $\Delta G_{cat}^{\ddagger}$ = 27.5 ± 3.3 kcal·mol^{-1} at 298 K. To our delight, these values compare well with those obtained for the reaction of **3** with benzene.

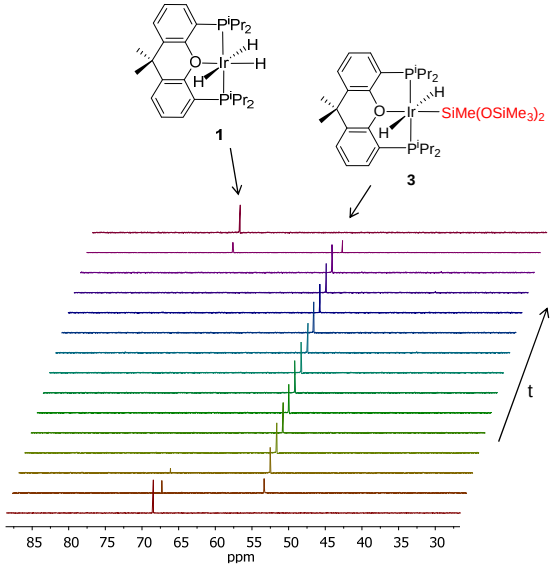

Figure 10. Stacked ^{31}P{^{1}H} NMR spectra (121.4 MHz, benzene, 358 K) showing the course of the catalytic silylation as a function of the time.

Table 3. Rate Constants for the Catalytic Silylation of Benzene (k_{cat}^{obs}).[a]

T (K)	k_{cat}^{obs} x 10^{-5} (s^{-1})
338	0.41 ± 0.08
343	0.76 ± 0.09
348	1.35 ± 0.10
353	1.94 ± 0.09

[a] [**1**]$_0$ = 0.028 M, [HSi] = 0.28 M, [cyclohexene] = 0.28 M.

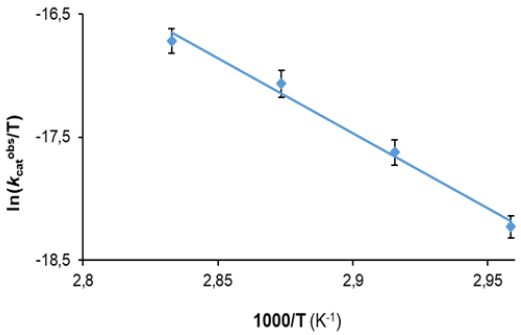

Figure 11. Eyring plot of the catalytic reaction of silylation of benzene.

The cycle shown in Scheme 9 significantly differs from that proposed for the iridium-phenanthroline catalysts. In contrast to the cycle shown in Scheme 2, hydride-disilyl species are not necessary for the catalysis, in our case. In both cycles, dihydride -silyl species participate, but their functions are different. While in the cycle shown in Scheme 2 it activates the Si-H bond of the silane, in our cycle it activates the C-H bond of the arene. The mechanism proposed for the iridium-phenanthroline catalysts and our mechanism are also different from that summarized in Scheme 3, for the borylation of arenes, but the three are consistent. In this context, it should be noted that the combination of the cycles shown in Schemes 2 and 9 formally give rise to the mechanism depicted on Scheme 3.

Trihydride **1** tolerates one of the widest varieties of functionalities, which includes CH_3, OCH_3, CF_3, F, Cl, and Br (Scheme 10).The selectivity of the functionalization is governed by steric factors, as expected for reactions controlled by the activation energy of the C-H bond cleavage of the arene. In this context, it should be mentioned that the activation energy for the rupture of a C-H bond depends upon two factors: the dissociation energy of the C-H bond and the stability of the σ-intermediate. So, because within an arene the strength of the different C-H bonds is generally similar, the difference in activation energy ($\Delta\Delta G^{\ddagger}$) between the distinct C-H bonds mainly depends on the stability of the respective σ-intermediates, which is governed by the steric hindrance experienced by the coordinated C-H bond. As a consequence, the C-H bond activation is kinetically controlled by steric factors; i.e., the less sterically hindered C-H bonds are generally the first activated ones. Thus, the functionalization takes place at the least sterically hindered C-H bonds of the aromatic ring. With the exception of fluorobenzene, monosubstituted benzenes give *meta*- and *para*-substituted products. The molar ratio between the isomers is modulated by the electronic nature of the substituent, increasing the *meta*:*para* ratio according to the sequence: MeO < Me < Cl < CF_3 ≈ Br; i.e., electron withdrawing groups disfavor the *para* isomer with regard to the donating substituents. 1,3-Disubstituted benzenes undergo exclusively silylation at position *meta* respect to both substituents. Fluorine atom shows a marked ability to approach the silyl group, in agreement with its well-known capacity to direct to *ortho* position the C-H bond activation of arenes, mediated by transition complexes.[28,39] Thus, fluorobenzene and 1,3-difluorobenzene give mixtures of the three possible isomers; particular mention merits the silylation of the latter,

which affords the silylated product bearing the silyl group situated *ortho* to one of the fluorine substituents and *para* to the other with high selectivity (70%). The reason of this fact appears to be related to an increase of the Si-C bond energy due to the *ortho*-fluorine substitution. The effect has been explained in terms of a rise of the ionic component of the bond by inductive effect of the fluorine atom.[40]

Scheme 10. Silylation of Arenes (%. Isolated Yields in Parentheses)

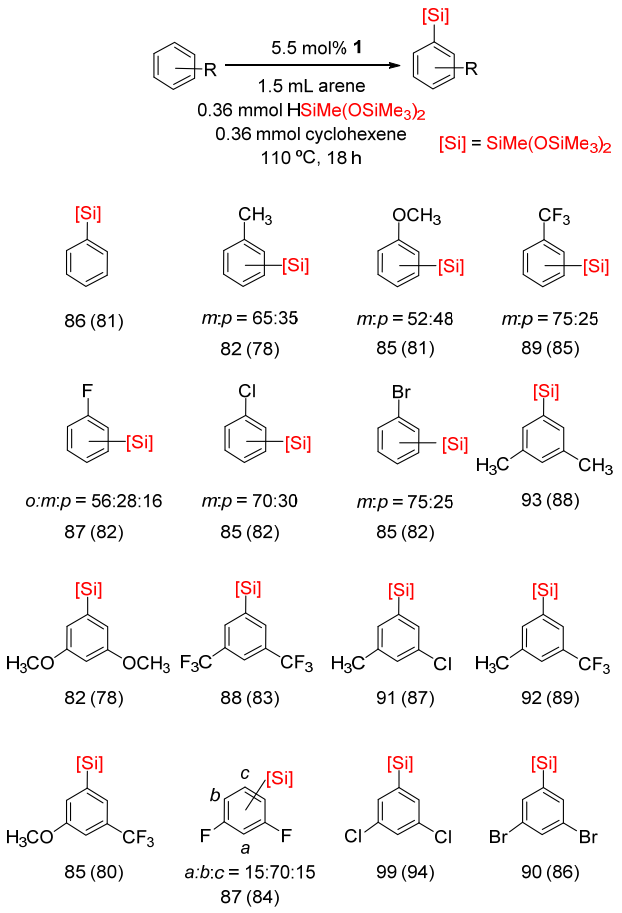

CONCLUDING REMARKS

This study reveals that the Si-H bond activation of silanes promoted by the trihydride $IrH_3\{\kappa^3\text{-P,O,P-[xant(P}^i\text{Pr}_2)_2]\}$ and the C-H bond activation of arenes mediated by dihydride-silyl derivatives of formulae $IrH_2(SiR_3)\{\kappa^3\text{-P,O,P-[xant(P}^i\text{Pr}_2)_2]\}$ can be sequenced in order to build catalytic reactions involving direct silylation of arenes mediated by the trihydride $IrH_3\{\kappa^3\text{-P,O,P-[xant(P}^i\text{Pr}_2)_2]\}$.

Stoichiometric isotopic labeling experiments as well as the results of a detailed kinetic study have demonstrated that the Si-H bond activation takes place through the σ-complexes $IrH_3(\eta^2\text{-H-SiR}_3)\{\kappa^2\text{-}cis\text{-P,P-[xant(P}^i\text{Pr}_2)_2]\}$ and that the oxidative addition of the coordinated bond to the metal center is the determining step of the activation.

Isotopic labeling experiments and kinetic results of the C-H bond activation indicate that it occurs through a classical mechanism where the C-H bond cleavage is the rate determining step. Its activation energy is higher than that of the Si-H bond activation. Thus, the C-H bond rupture is the rate determining step of the catalysis and, as consequence; the selectivity of the silylation of monosubstituted and 1,3-disubstituted arenes is generally governed by ligand-substrate steric interactions.

In summary, the catalytic cycle for the direct silylation of arenes catalyzed by a saturated polyhydride bearing a pincer ligand has been built, on the basis of stoichiometric isotopic labeling experiments, the kinetic analysis of the involved σ-bond activation reactions, and the full characterization of the key σ-intermediate for the Si-H bond activation.

EXPERIMENTAL SECTION

General Information. All reactions were carried out with exclusion of air using Schlenk-tube techniques or in a drybox. Instrumental methods and X-ray details are given in the Supporting Information. In the NMR spectra the chemical shifts (in ppm) are referenced to residual solvent peaks (^{1}H, ^{13}C{^{1}H}) or external 85% H_3PO_4 (^{31}P{^{1}H}), $SiMe_4$ (^{29}Si), or $CFCl_3$ (^{19}F). Coupling constants J and N ($N = J_{P\text{-}H} + J_{P'\text{-}H}$ for ^{1}H and $N = J_{P\text{-}C} + J_{P'\text{-}C}$ for ^{13}C{^{1}H}) are given in hertz.

Preparation of $IrH_2(SiEt_3)\{\kappa^3$-P,O,P-[xant(P^{i}Pr$_2$)$_2$]} (2). A solution of $IrH_3\{\kappa^3$-P,O,P-[xant(P^{i}Pr$_2$)$_2$]} (100 mg, 0.16 mmol) in toluene (3 mL) was treated with $HSiEt_3$ (25 µL, 0.16 mmol) and the resulting mixture was stirred at room temperature for 18 hours. After this time, the yellowish solution was evaporated to dryness to afford a yellow residue. Pentane was added to afford a white solid, which was washed with pentane (2 x 1 mL) and dried in vacuo. Yield: 65 mg (55%). Anal. Calcd. for $C_{33}H_{57}IrOP_2Si$: C, 52.70; H, 7.64. Found: C, 52.81; H, 7.59. HRMS (electrospray, *m/z*): calcd. for $C_{33}H_{56}SiIrOP_2$ $[M - H]^+$ 751.3200; found 751.3203. IR (cm^{-1}): ν(Ir-H) 1757 (w), ν(C-O-C) 1095 (m). ^{1}H NMR (300.13 MHz, C_6D_6, 298 K): δ 7.00 (m, 2H, CH-arom POP), 6.72 (d, $^3J_{H\text{-}H}$ = 7.5, 2H, CH-arom POP), 6.61 (t, $^3J_{H\text{-}H}$ = 7.5, 2H, CH-arom POP), 2.35 (m, 4H, PC*H*(CH$_3$)$_2$), 1.17 (dvt, $^3J_{H\text{-}H}$ = 7.2, N = 18.0, 24H, PCH(C*H*$_3$)$_2$), 1.04 (m, 6H, Si(C*H*$_2$CH$_3$)$_3$), 0.95 (m, 9H, Si(CH$_2$C*H*$_3$)$_3$, 0.90 (s, 6H, CH$_3$), –5.91 (t, $^2J_{H\text{-}P}$ = 17.4, 2H, Ir-H). ^{13}C{^{1}H} NMR (75.47 MHz, C_6D_6, 298 K): δ 156.8 (vt, N = 10.3, Carom), 132.5 (vt, N = 4.9, Carom), 129.7 (s, CH-arom), 125.9 (s, CH-arom), 125.0 (vt, N = 31.4, Carom), 124.3 (vt, N = 5.2, CH-arom), 34.4 (s, *C*(CH$_3$)$_2$), 28.9 (s, C(*C*H$_3$)$_2$), 26.0 (vt, N = 29.1, P*C*H(CH$_3$)$_2$), 19.5 (vt, N = 4.9, PCH(*C*H$_3$)$_2$), 18.4 (s, PCH(*C*H$_3$)$_2$), 14.9 (t, $^3J_{C\text{-}P}$ = 2.4, Si(*C*H$_2$CH$_3$)$_3$), 10.6 (s, Si(CH$_2$*C*H$_3$)$_3$). ^{31}P{^{1}H} NMR (121.49 MHz, C_6D_6, 298 K): δ 47.6 (s). ^{29}Si{^{1}H} NMR (59.63 MHz, C_6D_6, 298 K): δ -9.3 (t, $^2J_{Si\text{-}P}$ = 8.8).

Preparation of IrH_2[SiMe(OSiMe$_3$)$_2$]{κ^3-P,O,P-[xant(P^{i}Pr$_2$)$_2$]} (3). A solution of $IrH_3\{\kappa^3$-P,O,P-[xant(P^{i}Pr$_2$)$_2$]} (100 mg, 0.16 mmol) in toluene (3 mL) was treated with 1,1,1,3,5,5,5-heptamethyltrisiloxane (45 µL, 0.16 mmol) and the resulting mixture was stirred at room temperature for 18 hours. After this time, the yellowish solution was evaporated to dryness to afford a yellow residue. Pentane was added to afford a white solid, which was washed with cold pentane (2 x 1 mL) and dried in vacuo. Yield: 70 mg (49%). Anal. Calcd. for $C_{34}H_{63}IrO_3P_2Si_3$: C, 47.58; H, 7.40. Found: C, 47.58; H, 7.41. HRMS (electrospray, *m/z*): calcd. for $C_{34}H_{62}Si_3IrO_3P_2$ $[M-H]^+$ 857.3104; found 857.3135. IR (cm^{-1}): ν(Ir-H) 1758 (w), δ_s(Si-CH$_3$) 1246 (m), ν(C-O-C) 1033 (m). ^{1}H NMR (300.13 MHz, C_6D_6, 298 K): δ 7.24 (m, 2H, CH-

arom), 6.93 (d, $^3J_{H-H}$ = 7.5, 2H, CH-arom), 6.84 (t, $^3J_{H-H}$ = 7.5, 2H, CH-arom), 2.67 (m, 4H, PC*H*$(CH_3)_2$), 1.44 (dvt, $^3J_{H-H}$ = 7.5, *N* = 16.2, 12H, PCH(C*H*$_3)_2$), 1.21 (dvt, $^3J_{H-H}$ = 6.9, *N* = 13.8, 12H, PCH(C*H*$_3)_2$), 1.12 (s, 6H, CH_3), 0.79 (s, 3H, Si-*Me*$(OSiMe_3)_2$), 0.43 (s, 18H, SiMe(OSi*Me*$_3)_2$), –6.11 (t, $^2J_{H-P}$ = 17.1, 2H, Ir-H). $^{13}C\{^1H\}$ NMR (75.48 MHz, C_6D_6, 298 K): δ 156.6 (vt, *N* = 10.7, Carom), 133.2 (vt, *N* = 4.8, Carom), 130.2 (s, CH-arom), 126.4 (s, CH-arom), 125.6 (vt, *N* = 30.9, Carom), 124.4 (vt, *N* = 5.1, CH-arom), 34.4 (s, *C*$(CH_3)_2$), 29.8 (s, C(*C*$H_3)_2$), 25.8 (vt, *N* = 30.6, P*C*$H(CH_3)_2$), 19.4 (vt, *N* = 5.3, PCH(*C*$H_3)_2$), 18.3 (s, PCH(*C*$H_3)_2$), 15.5 (s, Si*Me*$(OSiMe_3)_2$), 3.2 (s, SiMe(OSi*Me*$_3)_2$). $^{31}P\{^1H\}$ NMR (161.99 MHz, C_6D_6, 298 K): δ 53.0 (s, triplet under off-resonance decoupling conditions). $^{29}Si\{^1H\}$ NMR (59.63 MHz, C_6D_6, 298 K): δ -7.9 (s, SiMe(O*Si*$Me_3)_2$), -58.2 (t, $^2J_{Si-P}$ = 10.9, *Si*$Me(OSiMe_3)_2$).

Preparation of $IrH_2(SiPh_3)\{\kappa^3$-P,O,P-[xant($P^iPr_2)_2$]} (4). A solution of $IrH_3\{\kappa^3$-P,O,P-[xant($P^iPr_2)_2$]} (100 mg, 0.16 mmol) in toluene (3 mL) was treated with $HSiPh_3$ (41 mg, 0.16 mmol) and the resulting mixture was stirred at room temperature for 18 hours. After this time, the yellowish solution was evaporated to dryness to afford a yellow residue. Pentane was added to afford a white solid, which was washed with pentane (2 x 1 mL) and dried in vacuo. Yield: 72 mg (51%). Anal. Calcd. for $C_{45}H_{57}IrOP_2Si$: C, 60.31; H, 6.41. Found: C, 60.08; H, 6.56. HRMS (electrospray, *m*/*z*): calcd. for $C_{45}H_{56}SiIrOP_2$ $[M-H]^+$ 895.3201; found 895.3177. IR (cm^{-1}): ν(Ir-H) 1772 (w), ν(C-O-C) 1087 (m). ^1H NMR (300.13 MHz, C_6D_6, 298 K): δ 8.39 (d, $^3J_{H-H}$ = 7.2, 6H, $SiPh_3$), 7.29 (t, $^3J_{H-H}$ = 7.2, 6H, $SiPh_3$), 7.18 (m, 3H, $SiPh_3$), 7.01 (m, 2H, CH-arom POP), 6.94 (d, $^3J_{H-H}$ = 7.5, 2H, CH-arom), 6.81 (t, $^3J_{H-H}$ = 7.5, 2H, CH-arom POP), 1.59 (m, 4H, PC*H*$(CH_3)_2$), 1.16 (s, 6H, CH_3), 1.02 (dvt, $^3J_{H-H}$ = 7.2, *N* = 13.8, 24H, PCH(C*H*$_3)_2$), –5.28 (t, $^2J_{H-P}$ = 16.8, 2H, Ir-H). $^{13}C\{^1H\}$ NMR (75.47 MHz, C_6D_6, 298 K): δ 156.8 (vt, *N* = 10.6, Carom), 144.4 (s, C $SiPh_3$), 138.5 (s, CH $SiPh_3$), 132.4 (vt, *N* = 4.8, Carom), 129.8 (s, CH-arom), 127.1 (s, CH $SiPh_3$), 125.9 (s, CH $SiPh_3$), 125.7 (s, CH-arom), 125.0 (vt, *N* = 31.0, Carom), 124.2 (vt, *N* = 5.6, CH-arom), 34.2 (s, *C*$(CH_3)_2$), 28.6 (br s, C(*C*$H_3)_2$), 23.6 (vt, *N* = 30.1, P*C*$H(CH_3)_2$), 18.7 (vt, *N* = 5.1, PCH(*C*$H_3)_2$), 17.3 (s, PCH(*C*$H_3)_2$). $^{31}P\{^1H\}$ NMR (121.49 MHz, C_6D_6, 298 K): δ 44.9 (s). $^{29}Si\{^1H\}$ NMR (59.63 MHz, C_6D_6, 298 K): δ -25.5 (t, $^2J_{Si-P}$ = 10.4).

Spectroscopic Characterization of $IrH_3(\eta^2$-H-$SiEt_3)\{\kappa^2$-*cis*-P,P-[xant($P^iPr_2)_2$]} (A_{SiEt3}). In the glovebox, an NMR tube was charged with a solution of **1** (10 mg, 0.016 mmol), $HSiEt_3$ (3 μL, 0.02 mmol) in toluene-d_8 (0.42 mL), and the NMR spectra of the resulting solution were recorded immediately. ^1H NMR (400.13 MHz, C_7D_8, 298 K): δ 7.01 (m, 4H, CH-arom POP), 6.91 (t, J_{H-H} = 7.6, 2H, CH-arom POP), 2.38 (m, 4H, PC*H*$(CH_3)_2$), 1.39 (s, 6H, CH_3), 1.28 (dd, $^3J_{H-H}$ = 7.6, $^3J_{H-P}$ = 15.2, 12H, PCH(C*H*$_3)_2$), 1.13 (dd, $^3J_{H-H}$ = 7.2, $^3J_{H-P}$ = 12.8, 12H, PCH(C*H*$_3)_2$), 0.96 (m, 6H, Si(C*H*$_2$CH$_3)_3$), 0.79 (m, 9H, Si(CH$_2$C*H*$_3)_3$, -12.09 (br, 4H, Ir-H). ^1H NMR (500.13 MHz, C_7D_8, 183 K, high field region, relative intensities): δ -9.73 (m, 3, Ir-H), -9.99 (m, 1, Ir-H), -11.19 (t, $^2J_{H-P}$ = 15.5, 2, Ir-H), -12.49 (dd, $^2J_{H-P}$ = 15.5, $^2J_{H-P}$ = 104, 2, Ir-H), -14.04 (m, 2, Ir-H), -14.33 (dd, $^2J_{H-P}$ = 21, $^2J_{H-P}$ = 111, 2, Ir-H). $^1H\{^{31}P\}$ NMR (500.13 MHz, C_7D_8, 183 K, high field region, relative intensities): δ -9.73 (br s, 3, Ir-H), -9.99 (br s, 1, Ir-H), -11.19 (br s, 2, Ir-H), -12.60 (br s, 2, Ir-H), -14.12 (br s, 2, Ir-H), -14.40 (br s, 2, Ir-H). $^{31}P\{^1H\}$ NMR (202.46 MHz, C_7D_8, 298 K): δ -1.2 (br s). $^{31}P\{^1H\}$ NMR (202.46 MHz, C_7D_8, 183 K): δ 8.7 (d, $^2J_{P-P}$ = 18.1), -5.9 (d, $^2J_{P-P}$ = 18.1), -12.8 (br s). $^{29}Si\{^1H\}$ NMR (99.36 MHz, C_7D_8, 183 K): δ 2.8 (br).

Reaction of $IrH_3\{\kappa^3$-P,O,P-[xant($P^iPr_2)_2$]} (1) with $DSiEt_3$. Two Wilmad screw-cap NMR tubes were charged with **1** (10 mg, 0.016 mmol). To the first NMR tube was added 0.42 mL of toluene and to the second was added 0.42 mL of toluene-d_8. $DSiEt_3$ (3 μL, 0.02 mmol) was added to both samples and they were periodically checked by NMR spectroscopy. After 28 h, the ^1H and ^2H NMR spectra showed the presence of **2** and **2-*d*$_1$**. The ^1H NMR (300.13 MHz, C_7D_8, 298 K) data were identical to those reported for **2** with the exception of the decrease of the intensity of the triplet at -5.76 ppm ($^2J_{H-P}$ = 17.4 Hz) corresponding to IrH_2 and the appearance of a new triplet at -5.61 ppm ($^2J_{H-P}$ = 17.4 Hz) corresponding to the IrHD isotopomer, being the deuterium incorporation at the hydride positions 25%. ^2H NMR (46.07 MHz, toluene, 298 K): δ -5.63 (s, IrD).

NMR Spectroscopic Study of the Transformation of $IrH_3\{\kappa^3$-P,O,P-xant($P^iPr_2)_2$} (1) into $A_{SiMe(OSiMe3)2}$ and $IrH_2[SiMe(OSiMe_3)_2]\{\kappa^3$-P,O,P-[xant($P^iPr_2)_2$]} (3). The experimental procedure is described for a particular case, but the same method was used in all experiments, which were run in duplicate. In the glovebox, an NMR tube was charged with a solution of **1** (10 mg, 0.016 mmol), 1,1,1,3,5,5,5-heptamethyltrisiloxane (129 μL, 0.47 mmol) in toluene (0.42 mL), and a capillary tube filled with a solution of the internal standard (PPh_3) in benzene-d_6 was placed in the NMR tube. The tube was immediately introduced into an NMR probe preheated at the desired temperature, and the reaction was monitored by $^{31}P\{^1H\}$ NMR at different intervals of time.

Determination of the Reaction Order for 1,1,1,3,5,5,5-heptamethyltrisiloxane in the Transformation of ***1*** *into* $A_{SiMe(OSiMe3)2}$. The experimental procedure is analogous to that described for the transformation of **1** into $A_{SiMe(OSiMe3)2}$ and **3**, starting form **1** (10 mg, 0.016 mmol, 0.0373 M) and variable concentrations of 1,1,1,3,5,5,5-heptamethyl trisiloxane (from 0.747 to 1.495 M) in toluene (0.42 mL). The experiments were carried out at 288 K.

NMR Spectroscopic Study of the Transformation of $IrH_2[SiMe(OSiMe_3)_2]\{\kappa^3$-P,O,P-[xant($P^iPr_2)_2$]} (3) into $IrH_3\{\kappa^3$-P,O,P-xant($P^iPr_2)_2$} (1). The experimental procedure is described for a particular case, but the same method was used in all experiments, which were run in duplicate. In the glovebox, an NMR tube was charged with a solution of **3** (14 mg, 0.016 mmol) in benzene (0.42 mL), and a capillary tube filled with a solution of the internal standard (PPh_3) in benzene-d_6 was placed in the NMR tube. The tube was immediately introduced into an NMR probe preheated at the desired temperature, and the reaction was monitored by $^{31}P\{^1H\}$ NMR at different intervals of time.

NMR Spectroscopic Study of the Catalysis. In the glovebox, an NMR tube was charged with a solution of **1** (15 mg, 0.023 mmol), 1,1,1,3,5,5,5-heptamethyltrisiloxane (64 μL, 0.23 mmol), cyclohexene (24 μL, 0.23 mmol) in benzene (0.42 mL). The tube was introduced into an NMR probe preheated at 85°C, and the reaction was monitored by $^{31}P\{^1H\}$ NMR at different intervals of time.

Determination of the Activation Parameters of the Catalytic Silylation of Benzene. The experimental procedure is described for a particular case, but the same method was used in all experiments, which were run in duplicate. In the glovebox, an NMR tube was charged with a solution of **1** (7.7 mg,

0.012 mmol), 1,1,1,3,5,5,5-heptamethyltrisiloxane (33 μL, 0.12 mmol), cyclohexene (12 μL, 0.12 mmol) in benzene (0.42 mL), and a capillary tube filled with a solution of 1,4-dioxane (used as internal standard) in benzene-d_6 was placed in the NMR tube. The tube was immediately introduced into an NMR probe preheated at the desired temperature, and the reaction was monitored by ^{1}H NMR at different intervals of time (a d1 = 10 sec was used in order ensure accurate integration of the signals).

General procedure for the Silylation Reactions. In an argon-filled glovebox an Ace pressure tube was charged with **1** (12.7 mg, 0.02 mmol), $HSiMe(OSiMe_3)_2$ (100 μL, 0.36 mmol), cyclohexene (33 μL, 0.36 mmol), pentadecane (10 μL, 0.036 mmol), as internal standard, and 1.5 mL of the arene. The resulting mixture was stirred at 110 °C for 18 h. After this time the yield of the silylation reaction was determined by GC on an Agilent Technologies 6890N gas chromatograph with a flame ionization detector, using an HP-Innowax column (30 m x 0.25 mm; film thickness 0.25 μm). The injector temperature was 250 °C, and the FID temperature was 300 °C. The oven temperature began at 60 °C for 5 min, then 15 °C per minute to 200 °C, and finally 200 °C for 13 min. Then the arene was evaporated under reduced pressure to afford a crude reaction mixture. The identity of the silylation product was confirmed by ^{1}H, ^{13}C{^{1}H}, and ^{29}Si{^{1}H} NMR spectroscopies, as well as by GC-MS analyses. The isolated yields were calculated after purification of the crude reaction mixture by flash chromatography over silica gel using diethyl ether as eluent and by evaporation to dryness.

ASSOCIATED CONTENT

Supporting Information. The Supporting Information is available free of charge on the ACS Publications web site.

Experimental details, NMR data of the silylation products, crystallographic data, computational details and energies of calculated complexes, and NMR spectra (PDF)

Cartesian coordinates of the optimized structures (XYZ)

Accession codes

CCDC 2014866 contains the crystallographic data for this paper. These data can be obtained free of charge via www.ccdc.cam.ac.uk/data_request/cif, or by e-mailing data_request@ccdc.cam.ac.uk, or by contacting The Cambridge Crystallographic Data Centre, 12 Union Road, Cambridge CB2 1EZ, UK; fax: +44 1223 336033

AUTHOR INFORMATION

Corresponding Author

* maester@unizar.es

Notes

The authors declare no competing financial interest.

ACKNOWLEDGMENT

Financial support from the MINECO of Spain (Projects CTQ2017-82935-P and RED2018-102387-T (AEI/FEDER, UE)), Gobierno de Aragón (Group E06_20R, project LMP148_18, and predoctoral contract to A.M.), FEDER, and the European Social Fund is acknowledged.

REFERENCES

(1) (a) Kubas, G. J. *Metal Dihydrogen and σ-Bond Complexes: Structure, Theory and Reactivity*; Kluwer: New York, 2001. (b) Kubas, G. J. Metal-dihydrogen and σ-bond coordination: the consummate extension of the Dewar-Chatt-Duncanson model for metal-olefin π bonding. *J. Organomet. Chem.* **2001**, *635*, 37-68. (c) Esteruelas, M. A.; López, A. M.; Oliván, M. Polyhydrides of Platinum Group Metals: Nonclassical Interactions and σ-Bond Activation Reactions. *Chem. Rev.* **2016**, *116*, 8770-8847. (d) Esteruelas, M. A.; Oliván, M.; Oñate, E. Sigma-bond activation reactions induced by unsaturated Os(IV)-hydride complexes. *Adv. Organomet. Chem.* **2020**, *74*, 53-104.

(2) (a) Cheng, C.; Hartwig, J. F. Catalytic Silylation of Unactivated C-H Bonds. *Chem. Rev.* **2015**, *115*, 8946-8975. (b) Yang, Y.; Wang C. Direct silylation reactions of inert C-H bonds via transition metal catalysis. *Sci. China Chem.* **2015**, *58*, 1266-1279. (c) Hartwig, J. F.; Romero, E. A. Iridium-catalyzed silylation of unactivated C-H bonds. *Tetrahedron* **2019**, *75*, 4059-4070. (d) Richter, S. C.; Oestreich, M. Emerging Strategies for C-H Silylation. *Trends Chem.* **2020**, *2*, 13-27.

(3) (a) Corey, J. Y. Reactions of Hydrosilanes with Transition Metal Complexes and Characterization of the Products. *Chem. Rev.* **2011,** *111,* 863-1071. (b) Corey, J. Y. Reactions of Hydrosilanes with Transition Metal Complexes. *Chem. Rev.* **2016**, *116*, 11291-11435.

(4) (a) Jones, W. D.; Feher, F. J. Comparative Reactivities of Hydrocarbon C-H Bonds with a Transition-Metal Complex. *Acc. Chem. Res.* **1989**, *22*, 91-100. (b) Shilov, A. E.; Shul'pin, G. B. Activation of C-H Bonds by Metal Complexes. *Chem. Rev.* **1997**, *97*, 2879-2932. (c) Balcells, D.; Clot, E.; Eisenstein, O. C-H Bond Activation in Transition Metal Species from a Computational Perspective. *Chem. Rev.* **2010**, *110*, 749-823. (d) Eisenstein, O.; Milani, J.; Perutz, R. N. Selectivity of C-H Activation and Competition between C-H and C-F Bond Activation at Fluorocarbons. *Chem. Rev.* **2017**, *117*, 8710-8753. (e) Gunsalus, N. J.; Koppaka, A.; Park, S. H.; Bischof, S. M.; Hashiguchi, B. G.; Periana, R. A. Homogeneous Functionalization of Methane. *Chem. Rev.* **2017**, *117*, 8521-8573. (f) Esteruelas, M. A.; Oliván, M. C-H Activation Coupling Reactions, in *Applied Homogeneous Catalysis with Organometallic Compounds: A Comprehensive Handbook in Four Volumes* 3rd Edition (B. Cornils, W. A. Herrmann, M. Beller, R. Paciello, Eds), Wiley, **2017**, chapter 23, 1307-1332. (g) Zhao, Q.; Meng, G.; Nolan, S. P.; Szostak, M. N‑Heterocyclic Carbene Complexes in C-H Activation Reactions. *Chem. Rev.* **2020**, *120*, 1981-2048.

(5) Nikonov, G. I. Recent Advances in Nonclassical Interligand Si···H Interactions. *Adv. Organomet. Chem.* **2005**, *53*, 217-309. (b) Lachaize, S.; Sabo-Etienne, S. σ-Silane Ruthenium Complexes: The Crucial Role of Secondary Interactions. *Eur. J. Inorg. Chem.* **2006**, *2006*, 2115-2127.

(6) (a) Bart, S. C.; Lobkovsky, E.; Chirik, P. J. Preparation and Molecular and Electronic Structures of Iron(0) Dinitrogen and Silane Complexes and Their Application to Catalytic Hydrogenation and Hydrosilation. *J. Am. Chem. Soc.* **2004**, *126*, 13794-13807. (b) Taw, F. L.; Bergman, R. G.; Brookhart, M. Silicon-Hydrogen Bond Activation and Formation of Silane Complexes Using a Cationic Rhodium(III) Complex. *Organometallics* **2004**, *23,* 886-890. (c) Matthews, S. L.; Pons, V.; Heinekey, D. M. Silane Complexes of Electrophilic Metal Centers. *Inorg. Chem.* **2006**, *45*, 6453-6459. (d) Vyboishchikov, S. F.; Nikonov, G. I. Rhodium Silyl Hydrides in Oxidation State +5: Classical or Nonclassical? *Organometallics* **2007**, *26,* 4160-4169. (e) McGrady, G. S.; Sirsch, P.; Chatterton, N. P.; Ostermann, A.; Gatti, C.; Altmannshofer, S.; Herz, V.; Eickerling, G.; Scherer, W. Nature of the Bonding in Metal-Silane *σ*-Complexes. *Inorg. Chem.* **2009**, *48*, 1588-1598. (f) Gutsulyak, D. V.; Vyboishchikov, S. F.; Nikonov, G. I. Cationic Silane *σ*-Complexes of Ruthenium with Relevance to Catalysis. *J. Am. Chem. Soc.* **2010**, *132*, 5950-5951. (g) Scherer, W.; Meixner, P.; Barquera-Lozada, J. E.; Hauf, C.; Obenhuber, A.; Brück, A.; Wolstenholme, D. J.; Ruhland, K.; Leusser, D.; Stalke, D. A Unifying Bonding Concept for Metal Hydrosilane Complexes. *Angew. Chem. Int. Ed.* **2013**, *52*, 6092-6096. (h) Komuro, T.; Arai, T.; Kikuchi, K.; Tobita, H. Synthesis of Ruthenium Complexes with a Nonspectator Si,O,P Chelate Ligand: Interconversion between

a Hydrido(η^2-silane) Complex and a Silyl Complex Leading to Catalytic Alkene Hydrogenation. *Organometallics* **2015**, *34*, 1211-1217. (i) Mai, V. H.; Korobkov, I.; Nikonov, G. I. Half-Sandwich Silane σ-Complexes of Ruthenium Supported by NHC Carbene. *Organometallics* **2016**, *35*, 936-942. (j) Price, J. S.; Emslie, D. J. H.; Berno, B. Manganese Silyl Dihydride Complexes: A Spectroscopic, Crystallographic, and Computational Study of Nonclassical Silicate and Hydrosilane Hydride Isomers. *Organometallics* **2019**, *38*, 2347-2362.

(7) Klare, H. F. T.; Oestreich, M.; Ito, J.; Nishiyama, H.; Ohki, Y.; Tatsumi, K. Cooperative Catalytic Activation of Si-H Bonds by a Polar Ru-S Bond: Regioselective Low-Temperature C-H Silylation of Indoles under Neutral Conditions by a Friedel-Crafts Mechanism. *J. Am. Chem. Soc.* **2011**, *133*, 3312-3315.

(8) (a) Sakakura, T.; Tokunaga, Y.; Sodeyama, T.; Tanaka, M. Catalytic C-H Activation. Silylation of Arenes with Hydrosilane or Disilane by $RhCl(CO)(PMe_3)_2$ under Irradiation. *Chem. Lett.* **1987**, 2375-2378. (b) Ezbiansky, K.; Djurovich, P. I.; LaForest, M.; Sinning, D. J.; Zayes, R.; Berry, D. H. Catalytic C-H Bond Functionalization: Synthesis of Arylsilanes by Dehydrogenative Transfer Coupling of Arenes and Triethylsilane. *Organometallics* **1998**, *17,* 1455-1457. (c) Cheng, C.; Hartwig, J. F. Rhodium-Catalyzed Intermolecular C-H Silylation of Arenes with High Steric Regiocontrol. *Science* **2014**, *343*, 853-857. (d) Cheng, C.; Hartwig, J. F. Mechanism of the Rhodium-Catalyzed Silylation of Arene C-H Bonds. *J. Am. Chem. Soc.* **2014**, *136*, 12064-12072. (e) Lee, K.; Katsoulis, D.; Choi, J. Intermolecular C-H Silylation of Arenes and Heteroarenes with $HSiEt_3$ under Operationally Diverse Conditions: Neat/Stoichiometric and Acceptor/Acceptorless. *ACS Catal.* **2016**, *6*, 1493-1496.

(9) (a) Gustavson, W. A.; Epstein, P. S.; Curtis, M. D. Homogeneous Activation of the C-H Bond Formation of Phenylsiloxanes from Benzene and Silicon Hydrides. *Organometallics* **1982**, *1*, 884-885. (b) Ishiyama, T.; Sato, K.; Nishio, Y.; Miyaura, N. Direct Synthesis of Aryl Halosilanes through Iridium(I)-Catalyzed Aromatic C-H Silylation by Disilanes, *Angew. Chem. Int. Ed.* **2003**, *42*, 5346-5348. (c) Ishiyama, T.; Sato, K.; Nishio, Y.; Saiki, T.; Miyaura, N. Regioselective aromatic C-H silylation of five-membered heteroarenes with fluorodisilanes catalyzed by iridium(I) complexes. *Chem. Commun.* **2005**, 5065-5067. (d) Saiki, T.; Nishio, Y.; Ishiyama, T.; Miyaura, N. Improvements of Efficiency and Regioselectivity in the Iridium(I)-Catalyzed Aromatic C-H Silylation of Arenes with Fluorodisilanes. *Organometallics* **2006**, *25,* 6068-6073. (e) Lu, B.; Falck, J. R. Efficient Iridium-Catalyzed C-H Functionalization/Silylation of Heteroarenes. *Angew. Chem. Int. Ed.* **2008**, *47*, 7508-7510. (f) Ishiyama, T.; Saiki, T.; Kishida, E.; Sasaki, I.; Ito, H.; Miyaura, N. Aromatic C-H silylation of arenes with 1-hydrosilatrane catalyzed by an iridium(I)/2,9-dimethylphenanthroline (dmphen) complex. *Org. Biomol. Chem.* **2013**, *11*, 8162-8165. (g) Minami, Y.; Komiyama, T.; Hiyama, T. Straightforward Synthesis of HOMSi Reagents via sp^2 C-H Silylation. *Chem. Lett.* **2015**, *44*, 1065-1067. (h) Murai, M.; Takami, K.; Takeshima, H.; Takai, K. Iridium-Catalyzed Dehydrogenative Silylation of Azulenes Based on Regioselective C-H Bond Activation. *Org. Lett.* **2015**, *17*, 1798-1801. (i) Cheng, C.; Hartwig, J. F. Iridium-Catalyzed Silylation of Aryl C-H Bonds. *J. Am. Chem. Soc.* **2015**, *137*, 592-595. (j) Murai, M.; Takami, K.; Takai, K. Iridium-Catalyzed Intermolecular Dehydrogenative Silylation of Polycyclic Aromatic Compounds without Directing Groups. *Chem. Eur. J.* **2015**, *21*, 4566-4570. (k) Rubio-Pérez, L.; Iglesias, M.; Munárriz, J.; Polo, V.; Passarelli, V.; Pérez-Torrente, J. J.; Oro, L. A. A well-defined NHC-Ir(III) catalyst for the silylation of aromatic C-H bonds: substrate survey and mechanistic insights. *Chem. Sci.* **2017**, *8*, 4811-4822. (l) Karmel, C.; Chen, Z.; Hartwig, J. F. Iridium-Catalyzed Silylation of C-H Bonds in Unactivated Arenes: A Sterically Encumbered Phenanthroline Ligand Accelerates Catalysis. *J. Am. Chem. Soc.* **2019**, *141*, 7063-7072. (m) Karmel, C.; Rubel, C. Z.; Kharitonova, E. V.; Hartwig, J. F. Iridium-Catalyzed Silylation of Five-Membered Heteroarenes: High Sterically Derived Selectivity from a Pyridyl-Imidazoline Ligand. *Angew. Chem. Int. Ed.* **2020**, *59*, 6074-6081. (n) Karmel, C.; Hartwig, J. F. Mechanism of the Iridium-Catalyzed Silylation of Aromatic C-H Bonds. *J. Am. Chem. Soc.* **2020**, *142*, 10494-10505.

(10) (a) Ishikawa, M.; Okazaki, S.; Naka, A.; Sakamoto, H. Nickel-Catalyzed Reactions of 3,4-Benzo-1,1,2,2-tetraethyl-1,2-disilacyclobutene with Aromatic Compounds. *Organometallics* **1992**, *11*, 4135-4139. (b) Ishikawa, M.; Sakamoto, H.; Okazaki, S.; Naka, A. Nickel-catalyzed reactions of 3,4-benzo-1,1,2,2-tetraethyl-1,2-disilaclobutene. *J. Organomet. Chem.* **1992**, *439*, 19-21. (c) Naka, A.; Lee, K. K.; Yoshizawa, K.; Yamabe, T.; Ishikawa, M. Nickel-Catalyzed Reactions of Benzo[1,2:4,5]bis(1,1,2,2-tetraethyl-1,2-disilacyclobut-3-ene) with Alkynes and Ketones. *Organometallics* **1999**, *18,* 4524-4529.

(11) (a) Uchimaru, Y.; El Sayed, A. M. M.; Tanaka, M. Selective Arylation of a Si-H Bond in *o*-Bis(dimethylsilyl)benzene via C-H Bond Activation of Arenes. *Organometallics* **1993**, *12*, 2065-2069. (b) Tsukada, N.; Hartwig, J. F. Intermolecular and Intramolecular, Platinum-Catalyzed, Acceptorless Dehydrogenative Coupling of Hydrosilanes with Aryl and Aliphatic Methyl C-H Bonds. *J. Am. Chem. Soc.* **2005**, *127*, 5022-5023. (c) Murata, M.; Fukuyama, N.; Wada, J.-I.; Watanabe, S.; Masuda, Y. Platinum-catalyzed Aromatic C-H Silylation of Arenes with 1,1,1,3,5,5,5-Heptamethyltrisiloxane. *Chem. Lett.* **2007**, *36*, 910-911.

(12) Xu, W.; Teng, H.; Luo, Y.; Lou, S.; Nishiura, M.; Hou, Z. Rare-Earth-Catalyzed C-H Silylation of Aromatic Heterocycles with Hydrosilanes. *Chem Asian J.* **2020**, *15*, 753-756.

(13) (a) Khusnutdinova, J. R.; Milstein, D. Metal-Ligand Cooperation. *Angew. Chem. Int. Ed.* **2015**, *54*, 12236-12273. (b) Kumar, A.; Bhatti, T. M.; Goldman, A. S. Dehydrogenation of Alkanes and Aliphatic Groups by Pincer-Ligated Metal Complexes. *Chem. Rev.* **2017**, *117*, 12357-12384. (c) Valdés, H.; García-Eleno, M. A.; Canseco-Gonzalez, D.; Morales-Morales, D. Recent Advances in Catalysis with Transition-Metal Pincer Compounds. *ChemCatChem* **2018**, *10*, 3136-3172.

(14) Sangtrirutnugul, P.; Tilley, T. D. Silyl Derivatives of [Bis(8-quinolyl)methylsilyl]iridium(III) Complexes: Catalytic Redistribution of Arylsilanes and Dehydrogenative Arene Silylation. *Organometallics* **2007**, *26,* 5557-5568.

(15) Asensio, G.; Cuenca, A. B.; Esteruelas, M. A.; Medio-Simón, M.; Oliván, M.; Valencia, M. Osmium(III) Complexes with POP Pincer Ligands: Preparation from Commercially Available $OsCl_3 \cdot 3H_2O$ and Their X-ray Structures. *Inorg. Chem.* **2010**, *49*, 8665-8667.

(16) Esteruelas, M. A.; Oliván, M. Osmium Complexes with POP Pincer ligands, in *Pincer Compounds: Chemistry and Applications*, 1st edition; Morales-Morales, D. Ed, Elsevier: Amsterdam 2018.

(17) (a) Esteruelas, M. A.; Oliván, M.; Vélez, A. Xantphos-Type Complexes of Group 9: Rhodium versus Iridium. *Inorg. Chem.* **2013**, *52*, 5339-5349. (b) Alós, J.; Esteruelas, M. A.; Oliván, M.; Oñate, E.; Puylaert, P. C-H Bond Activation Reactions in Ketones and Aldehydes Promoted by POP-Pincer Osmium and Ruthenium Complexes. *Organometallics* **2015**, *34*, 4908-4921. (c) Esteruelas, M. A.; Fernández, I.; García-Yebra, C.; Martín, J.; Oñate, E. Elongated σ-Borane versus σ-Borane in Pincer-POP-Osmium Complexes. *Organometallics* **2017**, *36*, 2298-2307. (d) Curto, S. G.; Esteruelas, M. A.; Oliván, M.; Oñate, E.; Vélez, A. Selective C-Cl Bond Oxidative Addition of Chloroarenes to a POP-Rhodium Complex. *Organometallics* **2017**, *36*, 114-128. (e) Esteruelas, M. A.; Fernández, I.; Martínez, A.; Oliván, M.; Oñate, E.; Vélez, A. Iridium-Promoted B-B Bond Activation: Preparation and X-ray Diffraction Analysis of a *mer*-Tris(boryl) Complex. *Inorg. Chem.* **2019**, 58, 4712-4717. (f) Esteruelas, M. A.; Fernández, I.; García-Yebra, C.; Martín, J.; Oñate, E. Cycloosmathioborane Compounds: Other Manifestations of the Hückel Aromaticity. *Inorg. Chem.* **2019**, *58*, 2265-2269.

(18) Esteruelas, M. A.; García-Yebra, C.; Martín, J.; Oñate, E. *mer*, *fac*, and Bidentate Coordination of an Alkyl-POP Ligand in the Chemistry of Nonclassical Osmium Hydrides. *Inorg. Chem.* **2017**, *56*, 676-683.

(19) Antiñolo, A.; Esteruelas, M. A.; García-Yebra, C.; Martín, J.; Oñate, E.; Ramos, A. Reactions of an Osmium(IV)-Hydroxo Complex with Amino-Boranes: Formation of Boroxide Derivatives. *Organometallics* **2019**, *38*, 310-318.

(20) (a) Bakhmutov, V. I.; Bozoglian, F.; Gómez, K.; González, G.; Grushin, V. V.; Macgregor, S. A.; Martin, E.; Miloserdov, F. E.; Novikov, M. A.; Panetier, J. A.; Romashov, L. V. CF_3-Ph Reductive Elimination from [(Xantphos)Pd(CF_3)(Ph)]. *Organometallics* **2012**, *31*, 1315-1328. (b) Jover, J.; Miloserdov, F. M.; Benet-Buchholz, J.; Grushin, V. V.; Maseras, F. On the Feasibility of Nickel-Catalyzed Trifluoromethylation of Aryl Halides. *Organometallics* **2014**, *33*, 6531-6543. (c) Curto S. G.; de las Heras, L. A.; Esteruelas, M. A.; Oliván M.; Oñate, E.; Vélez, A. Reactions of POP-Pincer Rhodium(I)-Aryl Complexes with Small Molecules: Coordination Flexibility of the Ether Diphosphine. *Can J. Chem.*, DOI: 10.1139/cjc-2020-0061.

(21) Alós, J.; Bolaño, T.; Esteruelas, M. A.; Oliván, M.; Oñate, E.; Valencia, M. POP-Pincer Ruthenium Complexes: d^6 Counterparts of Osmium d^4 Species. *Inorg. Chem.* **2014**, *53*, 1195-1209.

(22) Alós, J.; Bolaño, T.; Esteruelas, M. A.; Oliván, M.; Oñate, E.; Valencia, M. POP-Pincer Osmium-Polyhydrides: Head-to-Head (*Z*)-Dimerization of Terminal Alkynes. *Inorg. Chem.* **2013**, *52*, 6199-6213.

(23) Esteruelas, M. A.; García-Yebra, C.; Martín, J.; Oñate, E. Dehydrogenation of Formic Acid Promoted by a Trihydride-Hydroxo-Osmium(IV) Complex: Kinetics and Mechanism. *ACS Catal.* **2018**, *8*, 11314-11323.

(24) Adams, G. M.; Colebatch, A. L.; Skornia, J. T.; McKay, A. I.; Johnson, H. C.; Lloyd-Jones, G. C.; Macgregor, S. A.; Beattie, N. A.; Weller, A. S. Dehydropolymerization of $H_3B{\cdot}NMeH_2$ To Form Polyaminoboranes Using [Rh(Xantphos-alkyl)] Catalysts. *J. Am. Chem. Soc.* **2018**, *140*, 1481-1495.

(25) Esteruelas, M. A.; Nolis, P.; Oliván, M.; Oñate, E.; Vallribera, A.; Vélez, A. Ammonia Borane Dehydrogenation Promoted by a Pincer-Square-Planar Rhodium(I) Monohydride: A Stepwise Hydrogen Transfer from the Substrate to the Catalyst. *Inorg. Chem.* **2016**, *55*, 7176-7181.

(26) Haibach, M. C.; Wang, D. Y.; Emge, T. J.; Krogh-Jespersen, K.; Goldman, A. S. (POP)Rh pincer hydride complexes: unusual reactivity and selectivity in oxidative addition and olefin insertion reactions. *Chem. Sci.* **2013**, *4*, 3683-3692.

(27) Esteruelas, M. A.; Oliván, M.; Vélez, A. POP-Pincer Silyl Complexes of Group 9: Rhodium versus Iridium. *Inorg. Chem.* **2013**, *52*, 12108-12119.

(28) Esteruelas, M. A.; Oliván, M.; Vélez, A. POP-Rhodium-Promoted C-H and B-H Bond Activation and C-B Bond Formation. *Organometallics* **2015**, *34*, 1911-1924.

(29) Esteruelas, M. A.; Oliván, M.; Vélez, A. Conclusive Evidence on the Mechanism of the Rhodium-Mediated Decyanative Borylation. *J. Am. Chem. Soc.* **2015**, *137*, 12321-12329.

(30) (a) Curto, S. G.; Esteruelas, M. A.; Oliván, M.; Oñate, E.; Vélez, A. *β*-Borylalkenyl *Z*-*E* Isomerization in Rhodium-Mediated Diboration of Nonfunctionalized Internal Alkynes. *Organometallics* **2018**, *37*, 1970-1978. (b) Curto, S. G.; Esteruelas, M. A.; Oliván, M.; Oñate, E. Rhodium-Mediated Dehydrogenative Borylation-Hydroborylation of Bis(alkyl)alkynes: Intermediates and Mechanism. *Organometallics* **2019**, *38*, 2062-2074. (c) Curto, S. G.; Esteruelas, M. A.; Oliván, M.; Oñate, E. Insertion of Diphenylacetylene into Rh-Hydride and Rh-Boryl Bonds: Influence of the Boryl on the Behavior of the *β*-Borylalkenyl Ligand. *Organometallics* **2019**, *38*, 4183-4192.

(31) Curto, S. G.; de las Heras, L. A.; Esteruelas, M. A.; Oliván, M.; Oñate, E. C(sp^3)-Cl Bond Activation Promoted by a POP-Pincer Rhodium(I) Complex. *Organometallics* **2019**, *38*, 3074-3083.

(32) Esteruelas, M. A.; Martínez, A.; Oliván, M.; Oñate, E. Direct C-H Borylation of Arenes Catalyzed by Saturated Hydride-Boryl-Iridium-POP Complexes: Kinetic Analysis of the Elemental Steps, *Chem. Eur. J.* **2020**, *26*, 12632-12644.

(33) Buil, M. L.; Esteruelas, M. A.; Fernández, I.; Izquierdo, S.; Oñate, E. Cationic Dihydride Boryl and Dihydride Silyl Osmium(IV) NHC Complexes: A Marked Diagonal Relationship. *Organometallics* **2013**, *32*, 2744-2752.

(34) See for example: (a) Bleeke, J. R.; Thananatthanachon, T.; Rath, N. P. Silapentadienyl-Iridium-Phosphine Chemistry. *Organometallics* **2008**, *27,* 2436-2446. (b) McBee, J. L.; Tilley, T. D. Synthesis and Reactivity of Iridium and Rhodium Silyl Complexes Supported by a Bipyridine Ligand. *Organometallics* **2009**, 28, 5072-5081. (c) Calimano, E.; Tilley, T. D. Synthesis and reactivity of rhodium and iridium alkene, alkyl and silyl complexes supported by a phenyl-substituted PNP pincer ligand. *Dalton Trans.* **2010**, *39*, 9250-9263. (d) Choi, G.; Tsurugi, H.; Mashima, K. Hemilabile *N*-Xylyl-*N*′-methylperimidine Carbene Iridium Complexes as Catalysts for C-H Activation and Dehydrogenative Silylation: Dual Role of *N*-Xylyl Moiety for ortho-C-H Bond Activation and Reductive Bond Cleavage. *J. Am. Chem. Soc.* **2013**, *135*, 13149-13161.

(35) See for example: Scherer, W.; Meixner, P.; Batke, K.; Barquera-Lozada, J. E.; Ruhland, K.; Fischer, A.; Eickerling, G.; Eichele, K. *J*(Si,H) Coupling Constants in Nonclassical Transition-Metal Silane Complexes. *Angew. Chem. Int. Ed.* **2016**, *55*, 11673-11677.

(36) Fast, C. D.; Jones, C. A. H.; Schley, N. D. Selectivity and Mechanism of Iridium-Catalyzed Cyclohexyl Methyl Ether Cleavage. *ACS Catal.* **2020**, *10*, 6450-6456.

(37) Connors, K. A. *Chemical Kinetics: The Study of Reaction Rates in Solution*; Wiley-VCH, 1990.

(38) Gómez-Gallego, M.; Sierra, M. A. Kinetic Isotope Effects in the Study of Organometallic Reaction Mechanisms. *Chem. Rev.* **2011**, *111*, 4857-4963.

(39) Kalläne, S. I.; Teltewskoi, M.; Braun, T.; Braun, B. C-H and C-F Bond Activations at a Rhodium(I) Boryl Complex: Reaction Steps for the Catalytic Borylation of Fluorinated Aromatics. *Organometallics* **2015**, *34*, 1156-1169.

(40) (a) Evans, M. E.; Burke, C. L.; Yaibuathes, S.; Clot, E.; Eisenstein, O.; Jones, W. D. Energetics of C-H Bond Activation of Fluorinated Aromatic Hydrocarbons Using a [Tp'Rh(CNneopentyl)] Complex. *J. Am. Chem. Soc.* **2009**, *131*, 13464-13473. (b) Clot, E.; Mégret, C.; Eisenstein, O.; Perutz, R. N. Exceptional Sensitivity of Metal-Aryl Bond Energies to *ortho*-Fluorine Substituents: Influence of the Metal, the Coordination Sphere, and the Spectator Ligands on M-C/H-CBond Energy Correlations. *J. Am. Chem. Soc.* **2009**, *131*, 7817-7827. (c) Tanabe, T.; Brennessel, W. W.; Clot, E.; Eisenstein, O.; Jones, W. D. Synthesis, structure, and reductive elimination in the series Tp'Rh(PR_3)(Ar^F)H; Determination of rhodium-carbon bond energies of fluoroaryl substituents. *Dalton Trans.* **2010**, *39*, 10495-10509.

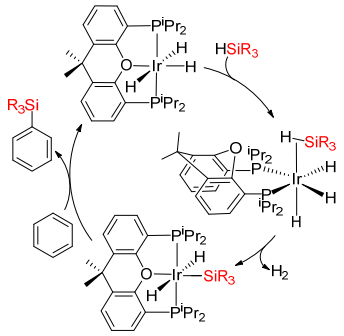
PiPr2
H
Ir
H
H
PiPr2
HSiR3
R3Si
H
SiR3
O
iPr2
P
Ir
H
P
iPr2
H
PiPr2
H
O
Ir
SiR3
H
PiPr2
H2